Application of current-algebra techniques to soft-pion production by the weak neutral current: S, P, T case*

Stephen L. Adler, E. W. Colglazier, Jr., J. B. Healy, Inga Karliner,
Judy Lieberman, Yee Jack Ng, and Hung-Sheng Tsao
The Institute for Advanced Study, Princeton, New Jersey 08540
(Received 23 June 1975)

We develop the cross-section formulas needed to correlate information on neutral currents obtained from deep-inelastic neutrino scattering, neutrino-proton elastic scattering, and neutral-current–induced soft-pion production, in the case of neutral currents with S, P, T spatial structure. (The necessary S, P, T current renormalization constants were estimated by us in a previous paper.) The pion-emission amplitude is obtained by current-algebra soft-pion techniques, with the effects of (3,3)-resonance excitation taken into account to leading nonvanishing order in the static approximation. We analyze recently reported Brookhaven National Laboratory results for neutral-current–induced soft-pion production under the simplifying assumption of a purely isoscalar S, P, T neutral current, while simultaneously imposing existing bounds on neutrino-proton elastic scattering and fitting existing data on neutral-current–induced deep-inelastic scattering. If all S P, T renormalization constants are given their central quark-model values, the elastic-scattering and deep-inelastic restrictions constrain the pion-production cross section to be too low compared with experiment; if apparently reasonable deviations of the parameters from the quark-model values are permitted, satisfactory fits to all data are obtained with S, T, with P, T or with S, P, T mixtures. An isovector tensor or pseudoscalar neutral current is found to lead to a strong (3,3) peak in πN invariant-mass plots, but an isovector scalar neutral current can be present without producing a visible (3,3) peak, even when ratios of the various πN charge states produced by the neutral current are appreciably changed from the values which they have in the isoscalar-current case. Two other interesting qualitative features of CP-conserving S, P, T structures are the following: (1) constructive T interference with S (or S and P) in $\nu + N \to \nu + N + \pi$ can accompany destructive interference in $\nu + p \to \nu + p$, and vice versa, and (ii) observation of unequal neutrino- and antineutrino-induced neutral-current cross sections would not be accompanied by neutral-current–induced parity-violating effects in the pp, ep, and μp interactions.

I. INTRODUCTION

Weak neutral-current experiments are now entering a new phase, in which substantial detailed information on the structure of the weak neutral interaction will be obtained in both inclusive and exclusive reactions. Ultimately, this should permit a determination of the phenomenological structure of the weak neutral interaction—either in favor of the conventionally assumed Weinberg-Salam phenomenology,[1] or some other combination of vector and axial-vector currents, or possibly in favor of an unconventional alternative.[2] In making this determination, it will be most important to correlate information about the three semileptonic reactions which will be studied in the greatest detail in the near future: deep-inelastic neutrino-nucleon scattering (in which the existence of neutral currents was first established[3]), neutrino-proton elastic scattering, and neutral-current–induced weak-pion production. The necessary apparatus for doing this in the case of the Weinberg-Salam model, and more generally for weak neutral currents formed solely from members of the usual vector and axial-vector (V,A) nonets, has already been developed.[4] This paper is the second of two devoted to setting up a similar apparatus for correlating inclusive and exclusive semileptonic neutral-current reactions in the case of neutral currents with scalar, pseudoscalar, and tensor (S,P,T) spatial structure. In the first paper,[5] the necessary renormalization constants describing nucleon and pion matrix elements of S,P,T current densities were estimated, using SU_3, chiral $SU(3)\times SU(3)$, and quark-model methods. In the present paper, we develop the necessary cross-section formulas for calculating neutrino-proton elastic scattering and especially neutrino-induced weak-pion production, and apply them to give sample fits to existing neutral-current data. In a subsequent paper[6] we will discuss in a similar fashion yet another alternative neutral-current structure, involving second-class V,A weak neutral currents.

The paper is organized as follows. In Sec. II we review the formulas for deep-inelastic inclusive neutrino-nucleon scattering in the S,P,T case, evaluate the cross section for neutrino-proton scattering, and finally apply current-algebra and static-model methods to calculate the pion-production cross section in the (3,3)-resonance region. In Sec. III we analyze low-invariant-mass [$W=M(\pi N)\leq 1.4$ GeV] pion production for the Brookhaven National Laboratory (BNL) flux spec-

trum, under the simplifying assumption of a pure isoscalar neutral current, and discuss some of the qualitative features of the sample S,P,T fits which are obtained. In Appendix A, we give the lengthy formulas for the pion-production amplitude and cross section, while in Appendix B we give details of the calculation of (3,3)-resonance excitation in the S,P,T case.

II. CROSS-SECTION FORMULAS

In this section we set up the cross-section formulas needed for correlating deep-inelastic inclusive and exclusive neutral-current–induced reactions in the S,P,T case. In Sec. IIA we give the necessary vertex structure and cross-section formulas needed to describe neutrino-nucleon elastic scattering. In Sec. IIB we give the formulas describing deep-inelastic scattering in the quark-parton picture. Finally, in Sec. IIC we develop the formulas needed to calculate pion production in the (3,3)-resonance region. Although the most general neutral-current phenomenology motivated by the quark model can contain both V,A and S,P,T couplings simultaneously, the fact that V,A couplings leave neutrino helicity unchanged while S,P,T couplings flip the neutrino helicity implies that amplitudes of the two classes cannot interfere (provided, as we shall assume throughout, that the neutrino mass is negligible relative to the initial and final neutrino energies). Hence differential cross sections are additive for each exclusive (or inclusive) channel,

$$d\sigma^{V,A,S,P,T} = d\sigma^{V,A} + d\sigma^{S,P,T}, \tag{1}$$

and so the formulas obtained below with only S,P,T couplings present, together with the V,A calculations of Ref. 4, suffice to describe the general case.

A. Elastic neutrino nucleon scattering

We shall consider in what follows the most general S,P,T neutral current which can be formed from members of the usual quark-model scalar, pseudoscalar, and tensor nonets. We start from the neutral-current effective Lagrangian[7]

$$\mathcal{L}^N_{\rm eff} = \frac{2G}{\sqrt{2}}\,(\bar\nu\nu\mathfrak{F} - \bar\nu\gamma_5\nu\mathfrak{F}^5 + \bar\nu\sigma_{\lambda\eta}\nu\mathfrak{F}^{\lambda\eta}), \tag{2}$$

with $\mathfrak{F}$, $\mathfrak{F}^5$, and $\mathfrak{F}^{\lambda\eta}$ being the hadronic scalar, pseudoscalar, and tensor currents. We assume Eq. (2) to be CP-conserving, which implies[8] that it is parity-conserving as well. Since experimentally the incoming neutrino is left-handed, the effective matrix element for accelerator neutrino reactions is obtained from Eq. (2) by making the substitution $\nu \to \frac{1}{2}(1-\gamma_5)\nu$, giving

$$\mathfrak{M}^N_{\rm eff} = \frac{G}{\sqrt{2}}[\,\bar\nu(1-\gamma_5)\nu(\mathfrak{F}+\mathfrak{F}^5) + \bar\nu\sigma_{\lambda\eta}(1-\gamma_5)\nu\mathfrak{F}^{\lambda\eta}]\,. \tag{3}$$

The most general quark-model structure for the scalar, pseudoscalar, and tensor currents is

$$\begin{aligned}
\mathfrak{F} &= g_{S0}\mathfrak{F}_0 + g_{S3}\mathfrak{F}_3 + g_{S8}\mathfrak{F}_8,\\
\mathfrak{F}^5 &= g_{P0}\mathfrak{F}^5_0 + g_{P3}\mathfrak{F}^5_3 + g_{P8}\mathfrak{F}^5_8\,,\\
\mathfrak{F}^{\lambda\eta} &= g_{T0}\mathfrak{F}^{\lambda\eta}_0 + g_{T3}\mathfrak{F}^{\lambda\eta}_3 + g_{T8}\mathfrak{F}^{\lambda\eta}_8,
\end{aligned} \tag{4}$$

with $\mathfrak{F}_j$, $\mathfrak{F}^5_j$, $\mathfrak{F}^{\lambda\eta}_j$ being first-class nonet currents represented in the quark model (with quark field ψ) by

$$\begin{aligned}
\mathfrak{F}_j &= \bar\psi\tfrac{1}{2}\lambda_j\psi,\\
\mathfrak{F}^5_j &= \bar\psi\gamma_5\tfrac{1}{2}\lambda_j\psi,\\
\mathfrak{F}^{\lambda\eta}_j &= \bar\psi\sigma^{\lambda\eta}\tfrac{1}{2}\lambda_j\psi.
\end{aligned} \tag{5}$$

The parameters g_{Sj}, g_{Pj}, g_{Tj}, $j=0,3,8$ are real numbers (complex if CP is not conserved). We express the nucleon matrix elements of the neutral members of these current nonets in the form[5]

$$\langle N(p_2)|\mathfrak{F}_j|N(p_1)\rangle = \mathfrak{N}_N\bar u(p_2)F_S^{(j)}(k^2)t_j\,u(p_1),$$

$$\langle N(p_2)|\mathfrak{F}^5_j|N(p_1)\rangle = \mathfrak{N}_N\bar u(p_2)F_P^{(j)}(k^2)\gamma_5 t_j u(p_1),$$

$$\begin{aligned}
\langle N(p_2)|\mathfrak{F}^{\lambda\eta}_j|N(p_1)\rangle &= \mathfrak{N}_N\bar u(p_2)\left[T_1^{(j)}(k^2)\sigma^{\lambda\eta} + i\,\frac{T_2^{(j)}(k^2)}{M_N}(\gamma^\lambda k^\eta - \gamma^\eta k^\lambda) + i\,\frac{T_3^{(j)}(k^2)}{M_N^2}(P^\lambda k^\eta - P^\eta k^\lambda)\right]t_j u(p_1)\\
&= \mathfrak{N}_N\bar u(p_2)\left[T_1^{(j)}(k^2)\sigma^{\lambda\eta} + i\,\frac{\hat T_2^{(j)}(k^2)}{M_N}(\gamma^\lambda k^\eta - \gamma^\eta k^\lambda) + \frac{T_3^{(j)}(k^2)}{M_N^2}(\sigma^{\lambda\nu}k_\nu k^\eta - \sigma^{\eta\nu}k_\nu k^\lambda)\right]t_j u(p_1),
\end{aligned} \tag{6}$$

$$\hat T_2^{(j)}(k^2) \equiv T_2^{(j)}(k^2) + 2T_3^{(j)}(k^2),$$

$$k = p_2 - p_1,\quad P = p_2 + p_1,\quad \mathfrak{N}_N = \left(\frac{M_N}{p_{20}}\,\frac{M_N}{p_{10}}\right)^{1/2},\quad t_3 = \tfrac{1}{2}\tau_3,\quad t_0 = \tfrac{1}{2}\left(\tfrac{2}{3}\right)^{1/2},\quad t_8 = \tfrac{1}{2}\left(\tfrac{1}{3}\right)^{1/2},$$

with τ_3 being the nucleon Pauli isospin matrix and with the spinors $\bar u(p_2)$, $u(p_1)$ understood to include

nucleon isospinors. (Second-class currents would imply one extra tensor form factor.)

Defining total form factors $F_S^T(k^2)$, $F_P^T(k^2)$, $T_{1,2,3}^T(k^2)$ by

$$\begin{aligned}
F_S^T(k^2) &= \tfrac{1}{2}(\tfrac{2}{3})^{1/2} g_{S0} F_S^{(0)}(k^2) + \tfrac{1}{2}\epsilon g_{S3} F_S^{(3)}(k^2) + \tfrac{1}{2}(\tfrac{1}{3})^{1/2} g_{S8} F_S^{(8)}(k^2),\\
F_P^T(k^2) &= \tfrac{1}{2}(\tfrac{2}{3})^{1/2} g_{P0} F_P^{(0)}(k^2) + \tfrac{1}{2}\epsilon g_{P3} F_P^{(3)}(k^2) + \tfrac{1}{2}(\tfrac{1}{3})^{1/2} g_{P8} F_P^{(8)}(k^2),\\
T_j^T(k^2) &= \tfrac{1}{2}(\tfrac{2}{3})^{1/2} g_{T0} T_j^{(0)}(k^2) + \tfrac{1}{2}\epsilon g_{T3} T_j^{(3)}(k^2) + \tfrac{1}{2}(\tfrac{1}{3})^{1/2} g_{T8} T_j^{(8)}(k^2),
\end{aligned} \tag{7}$$

with $\epsilon = 1$ for $\nu + p \to \nu + p$ and $\epsilon = -1$ for $\nu + n \to \nu + n$, the differential cross section for neutrino-nucleon scattering takes the form

$$\frac{d\sigma(\nu + N \to \nu + N)}{dt} = \frac{G^2}{8\pi E^2 M_N{}^2}\Sigma, \tag{8}$$

$$\begin{aligned}
\Sigma = \tfrac{1}{2}t \Big\{ &\tfrac{1}{2}(t + 4M_N{}^2)|F_S^{T\prime}|^2 + \tfrac{1}{2}t|F_P^T|^2 + 4\,\mathrm{Re}\,(F_S^{T\prime} T_2^{T*})(4M_N E - t) + \frac{2|T_2^T|^2}{M_N{}^2}[(4M_N E - t)^2 - t^2] \Big\}\\
&- \mathrm{Re}[(F_S^{T\prime} - F_P^T) T_1^{T*}]\, t(4M_N E - t) - 4\,\mathrm{Re}\,(T_2^T T_1^{T*}) t^2 + 2|T_1^T|^2[(4M_N E - t)^2 - 2M_N{}^2 t],
\end{aligned}$$

$$t = -k^2, \quad F_S^{T\prime} \equiv F_S^T + \frac{2T_3^T}{M_N{}^2}(4M_N E - t),$$

with E being the initial lab neutrino energy.

For incident antineutrinos, the sign of the tensor amplitudes T_j^T in Eq. (8) is reversed.

B. Deep inelastic inclusive neutrino nucleon scattering

We turn next to the formulas describing deep-inelastic neutrino-nucleon scattering. We use the standard spin-$\frac{1}{2}$ quark-parton model,[9] with the additional assumptions that the strange-parton, antiparton, and possible charmed-parton content of the nucleon may be neglected.[10] The quark-parton model in this form is expected to be good to an accuracy of order 20% for the quantities in which we are interested, and has the great virtue that all x dependence[11] (for an average nucleon target) appears in a single universal over-all factor which drops out in cross-section ratios. For the standard deep-inelastic neutrino-nucleon scattering ratios

$$\begin{aligned}
R_\nu &\equiv \frac{\sigma(\nu + N \to \nu + \Gamma)}{\sigma(\nu + N \to \mu^- + \Gamma)},\\
R_{\bar\nu} &\equiv \frac{\sigma(\bar\nu + N \to \bar\nu + \Gamma)}{\sigma(\bar\nu + N \to \mu^+ + \Gamma)},
\end{aligned} \tag{9}$$

we find[2]

$$\begin{aligned}
R_\nu &= \tfrac{1}{12}S_1 - \tfrac{2}{3}S_2 + \tfrac{14}{3}S_3,\\
R_{\bar\nu} &= \tfrac{1}{4}S_1 + 2S_2 + 14S_3,\\
S_1 &= [\tfrac{1}{2}(\tfrac{2}{3})^{1/2} g_{S0} + \tfrac{1}{2}(\tfrac{1}{3})^{1/2} g_{S8}]^2 + (\tfrac{1}{2}g_{S3})^2\\
&\quad + [\tfrac{1}{2}(\tfrac{2}{3})^{1/2} g_{P0} + \tfrac{1}{2}(\tfrac{1}{3})^{1/2} g_{P8}]^2 + (\tfrac{1}{2}g_{P3})^2,\\
S_2 &= [\tfrac{1}{2}(\tfrac{2}{3})^{1/2} g_{S0} + \tfrac{1}{2}(\tfrac{1}{3})^{1/2} g_{S8} - \tfrac{1}{2}(\tfrac{2}{3})^{1/2} g_{P0} - \tfrac{1}{2}(\tfrac{1}{3})^{1/2} g_{P8}]\\
&\quad \times [\tfrac{1}{2}(\tfrac{2}{3})^{1/2} g_{T0} + \tfrac{1}{2}(\tfrac{1}{3})^{1/2} g_{T8}] + (\tfrac{1}{2}g_{S3} - \tfrac{1}{2}g_{P3})\tfrac{1}{2}g_{T3},\\
S_3 &= [\tfrac{1}{2}(\tfrac{2}{3})^{1/2} g_{T0} + \tfrac{1}{2}(\tfrac{1}{3})^{1/2} g_{T8}]^2 + (\tfrac{1}{2}g_{T3})^2,
\end{aligned} \tag{10}$$

while for the normalized y distributions[11] for $\nu + N \to \nu + \Gamma$ and $\bar\nu + N \to \bar\nu + \Gamma$ we find respectively

$$\begin{aligned}
\frac{1}{\sigma_\nu}\frac{d\sigma_\nu}{dy} &= \frac{y^2 S_1 - 8y(1 - \frac{1}{2}y)S_2 + 32(1 - \frac{1}{2}y)^2 S_3}{\frac{1}{3}S_1 - \frac{8}{3}S_2 + \frac{56}{3}S_3},\\
\frac{1}{\sigma_{\bar\nu}}\frac{d\sigma_{\bar\nu}}{dy} &= \frac{y^2 S_1 + 8y(1 - \frac{1}{2}y)S_2 + 32(1 - \frac{1}{2}y)^2 S_3}{\frac{1}{3}S_1 + \frac{8}{3}S_2 + \frac{56}{3}S_3}.
\end{aligned} \tag{11}$$

C. Neutral-current pion production

We turn finally to the central subject of this paper, the calculation of pion production by the weak neutral interaction in the S,P,T coupling case. We employ the same basic pion-production model used to treat the V,A case in Ref. 4, where an assessment of the region of validity of the model is given. In this model, the pseudoscalar-coupling nucleon Born terms and pion-pole terms are included without kinematic approximations, with the dominant (3,3) multipoles unitarized so as to correctly describe (3,3)-resonance excitation. In addition, so-called "PCAC (partial conservation of axial-vector current) consistency condition" terms (the residual terms obtained after rearranging the nucleon Born terms from pseudovector to pseudoscalar form) and the current-algebra equal-time commutator term are added to the Born approximation and resonant terms, yielding a pion-production amplitude which has the correct soft-pion limit. When applied to the vector current in pion photoproduction and electroproduction, the model just described yields the basic CGLN-FNW (Chew-Goldberger-Low-Nambu-Fubini-Nambu-Wataghin) model[12] with soft pion corrections, and is in good[13,14] agreement with experiment in the low invariant mass

($W \leq 1.4$ GeV) region. Similarly, when applied to the V,A current case, the model gives a satisfactory account of low-invariant-mass pion production by the charged weak current.[14]

The formal starting point for our pion-production calculation is the standard soft-pion formula[15] for pion emission in the process $\mathcal{J}+N \to \pi^j+N$, with $\mathcal{J}$ being a general external current and N being a nucleon. This reads [with $\mathfrak{N}_{N\pi}=\mathfrak{N}_N(2q_0)^{-1/2}$]

$$\langle N(p_2)\pi(q)|\mathcal{J}(0)|N(p_1)\rangle = -\mathfrak{N}_{N\pi}\bar{u}(p_2)\Big[\frac{g_r}{M_N g_A}J_j'(k-q)+\frac{g_r}{2M_N}\{\gamma_5\tau_j, J(k)\}_+ + \frac{g_r}{2M_N}\gamma_5\tau_j\frac{\not p_2+\not q+M_N}{\nu-\nu_B}J(k)-J(k)\frac{(\not p_1-\not q+M_N)}{\nu+\nu_B}\frac{g_r}{2M_N}\gamma_5\tau_j + \text{possible additional pion-pole "seagull" contribution}\Big]u(p_1)\psi_j^* + O(q), \tag{12}$$

with

$$\nu=(p_1+p_2)\cdot k/(2M_N),\quad \nu_B=-q\cdot k/(2M_N),$$
$$\langle N(p_2)|\mathcal{J}(0)|N(p_1)\rangle = \mathfrak{N}_N\bar{u}(p_2)J(p_2-p_1)u(p_1), \tag{13}$$
$$\langle N(p_2)|[F_j^5,\mathcal{J}(0)]|N(p_1)\rangle = \mathfrak{N}_N\bar{u}(p_2)J_j'(p_2-p_1)u(p_1).$$

In Eqs. (12) and (13), $k=p_2+q-p_1$ denotes the four-momentum carried by the external current, $g_r \approx 13.5$ is the pion-nucleon coupling constant, and ψ_j is the isospin wave function of the emitted pion. The first term on the right-hand side of Eq. (12) is evidently the current-algebra equal-time commutator term, the second term (involving a γ- and τ-matrix anticommutator) is the "PCAC consistency condition" term, while the third and fourth terms are the usual pseudoscalar-coupling nucleon Born terms. The additional pion-pole "seagull" piece[16] is necessary only when the pion-pole contributions of the first four terms do not add up to give the full pion-pole contribution expected for the reaction $\mathcal{J}+N\to\pi^j+N$; we will see below that such a contribution is present in the isovector tensor amplitude.

As the first step in applying the recipe of Eq. (12) we calculate the needed equal-time commutators. Writing [cf. Eqs. (3) and (4)]

$$\mathcal{J}(0)=\mathcal{J}(0)^{S,P}+\mathcal{J}(0)^T,$$
$$\mathcal{J}(0)^{S,P}=\frac{G}{\sqrt{2}}\bar{\nu}(1-\gamma_5)\nu(g_{S0}\mathfrak{F}_0+g_{S3}\mathfrak{F}_3+g_{S8}\mathfrak{F}_8 + g_{P0}\mathfrak{F}_0^5+g_{P3}\mathfrak{F}_3^5+g_{P8}\mathfrak{F}_8^5), \tag{14}$$
$$\mathcal{J}(0)^T=\frac{G}{\sqrt{2}}\bar{\nu}\sigma_{\lambda\eta}(1-\gamma_5)\nu(g_{T0}\mathfrak{F}_0^{\lambda\eta}+g_{T3}\mathfrak{F}_3^{\lambda\eta}+g_{T8}\mathfrak{F}_8^{\lambda\eta})$$

and, in the tensor case, making repeated use of the identity

$$\frac{i}{2}\sigma_{\lambda\eta}\epsilon^{\lambda\eta}{}_{\mu\nu}=-\gamma_5\sigma_{\mu\nu}, \tag{15}$$

we find for the commutators

$$[F_j^5,\mathcal{J}(0)^{S,P}]=-\frac{G}{\sqrt{2}}\bar{\nu}(1-\gamma_5)\nu\{[(\tfrac{2}{3})^{1/2}g_{S0}+(\tfrac{1}{3})^{1/2}g_{S8}]\mathfrak{F}_j^5+g_{S3}\delta_{j3}[(\tfrac{2}{3})^{1/2}\mathfrak{F}_0^5+(\tfrac{1}{3})^{1/2}\mathfrak{F}_8^5] + [(\tfrac{2}{3})^{1/2}g_{P0}+(\tfrac{1}{3})^{1/2}g_{P8}]\mathfrak{F}_j+g_{P3}\delta_{j3}[(\tfrac{2}{3})^{1/2}\mathfrak{F}_0+(\tfrac{1}{3})^{1/2}\mathfrak{F}_8]\}, \tag{16}$$
$$[F_j^5,\mathcal{J}(0)^T]=\frac{G}{\sqrt{2}}\bar{\nu}\sigma_{\lambda\eta}(1-\gamma_5)\nu\{[(\tfrac{2}{3})^{1/2}g_{T0}+(\tfrac{1}{3})^{1/2}g_{T8}]\mathfrak{F}_j^{\lambda\eta}+g_{T3}\delta_{j3}[(\tfrac{2}{3})^{1/2}\mathfrak{F}_0^{\lambda\eta}+(\tfrac{1}{3})^{1/2}\mathfrak{F}_8^{\lambda\eta}]\}.$$

In evaluating the nucleon matrix elements of the tensor terms in Eqs. (15) and (16) an ambiguity occurs, since there is no *a priori* rule to tell us which of the two forms of the tensor vertex in Eq. (6) should be used. Although equivalent between on-shell nucleon spinors, the two vertex forms give different pion-production matrix elements when substituted into Eq. (12). Explicit calculation shows that the difference between the two matrix elements is

$$\langle N(p_2)\pi(q)|\mathcal{J}(0)|N(p_1)\rangle\big|_{\substack{\text{second form of}\\ \text{tensor vertex in}\\ \text{Eq. (6)}}} - \langle N(p_2)\pi(q)|\mathcal{J}(0)|N(p_1)\rangle\big|_{\substack{\text{first form of}\\ \text{tensor vertex}\\ \text{in Eq. (6)}}} = -\mathfrak{N}_{N\pi}\bar{u}(p_2)\Delta\mathfrak{M}_j u(p_1)\psi_j^*, \tag{17}$$
$$\Delta\mathfrak{M}_j=\frac{G}{\sqrt{2}}\bar{\nu}\sigma_{\lambda\eta}(1-\gamma_5)\nu\frac{g_r}{2M_N}\Big\{\frac{\not q}{2M_N}\gamma_5\tau_j,\sum_j g_{Tj}t_j\frac{2iT_3^{(j)}}{M_N}(\gamma^\lambda k^\eta-\gamma^\eta k^\lambda)\Big\}_+,$$

down by a factor[17] $\not q/(2M_N)$ relative to the leading T_3 contribution, which in turn is down by a factor k/M_N

relative to the leading tensor contribution coming from the intrinsic tensor term T_1. Hence the numerical effect of the ambiguity should be very small. In evaluating Eq. (12) we consistently use the second form of the tensor vertex given in Eq. (6), in which the dependence on the external nucleon four-momenta p_1 and p_2 occurs only through the neutrino four-momentum transfer $k = k_1 - k_2$.

Substituting Eqs. (6), (14), and (16) into Eq. (12) and neglecting $O(q)$ pion recoil corrections except where they occur in pion-pole terms, we get the following expression for the pion-production matrix element:

$$\langle N(p_2)\pi(q)|\mathcal{J}(0)|N(p_1)\rangle = -\mathfrak{N}_{N\pi}\bar{u}(p_2)(\mathfrak{M}_j^{S,P}+\mathfrak{M}_j^{T}+\mathfrak{M}_j^{T\pi})u(p_1)\psi_j^*, \tag{18}$$

$$\mathfrak{M}_j^{S,P}=\frac{G}{\sqrt{2}}\bar{\nu}(1-\gamma_5)\nu\left(\frac{-g_r}{M_N g_A}\{[(\tfrac{2}{3})^{1/2}g_{S0}+(\tfrac{1}{3})^{1/2}g_{S8}]t_jF_P^{(3)}((k-q)^2)\gamma_5+g_{S3}\delta_{j3}[(\tfrac{2}{3})^{1/2}t_0F_P^{(0)}(k^2)\gamma_5+(\tfrac{1}{3})^{1/2}t_8F_P^{(8)}(k^2)\gamma_5]\right.$$

$$+[(\tfrac{2}{3})^{1/2}g_{P0}+(\tfrac{1}{3})^{1/2}g_{P8}]t_jF_S^{(3)}(k^2)+g_{P3}\delta_{j3}[(\tfrac{2}{3})^{1/2}t_0F_S^{(0)}(k^2)+(\tfrac{1}{3})^{1/2}t_8F_S^{(8)}(k^2)]\}$$

$$+\frac{g_r}{2M_N}\left\{\gamma_5\tau_j,\sum_l t_l[g_{Sl}F_S^{(l)}(k^2)+g_{Pl}F_P^{(l)}(k^2)\gamma_5]\right\}_+$$

$$+\frac{g_r}{2M_N}\gamma_5\tau_j\frac{(\not p_2+\not q+M_N)}{\nu-\nu_B}\sum_l t_l[g_{Sl}F_S^{(l)}(k^2)+g_{Pl}F_P^{(l)}(k^2)\gamma_5]$$

$$\left.-\sum_l t_l[g_{Sl}F_S^{(l)}(k^2)+g_{Pl}F_P^{(l)}(k^2)\gamma_5]\frac{(\not p_1-\not q+M_N)}{\nu+\nu_B}\frac{g_r}{2M_N}\gamma_5\tau_j\right),$$

$$\mathfrak{M}_j^{T}=\frac{G}{\sqrt{2}}\bar{\nu}\sigma_{\lambda\eta}(1-\gamma_5)\nu\left(\frac{g_r}{M_N g_A}\left\{[(\tfrac{2}{3})^{1/2}g_{T0}+(\tfrac{1}{3})^{1/2}g_{T8}]t_j\left[T_1^{(3)}(k^2)\sigma^{\lambda\eta}+i\frac{\hat{T}_2^{(3)}(k^2)}{M_N}(\gamma^\lambda k^\eta-\gamma^\eta k^\lambda)+\frac{T_3^{(3)}(k^2)}{M_N^2}(\sigma^{\lambda\nu}k_\nu k^\eta-\sigma^{\eta\nu}k_\nu k^\lambda)\right]\right.\right.$$

$$+g_{T3}\delta_{j3}(\tfrac{2}{3})^{1/2}t_0\left[T_1^{(0)}(k^2)\sigma^{\lambda\eta}+i\frac{\hat{T}_2^{(0)}(k^2)}{M_N}(\gamma^\lambda k^\eta-\gamma^\eta k^\lambda)+\frac{T_3^{(0)}(k^2)}{M_N^2}(\sigma^{\lambda\nu}k_\nu k^\eta-\sigma^{\eta\nu}k_\nu k^\lambda)\right]$$

$$\left.\left.+g_{T3}\delta_{j3}(\tfrac{1}{3})^{1/2}t_8\left[T_1^{(8)}(k^2)\sigma^{\lambda\eta}+i\frac{\hat{T}_2^{(8)}(k^2)}{M_N}(\gamma^\lambda k^\eta-\gamma^\eta k^\lambda)+\frac{T_3^{(8)}(k^2)}{M_N^2}(\sigma^{\lambda\nu}k_\nu k^\eta-\sigma^{\eta\nu}k_\nu k^\lambda)\right]\right\}\right.$$

$$+\frac{g_r}{2M_N}\left\{\gamma_5\tau_j,\sum_l g_{Tl}t_l\left[T_1^{(l)}(k^2)\sigma^{\lambda\eta}+i\frac{\hat{T}_2^{(l)}(k^2)}{M_N}(\gamma^\lambda k^\eta-\gamma^\eta k^\lambda)+\frac{T_3^{(l)}(k^2)}{M_N^2}(\sigma^{\lambda\nu}k_\nu k^\eta-\sigma^{\eta\nu}k_\nu k^\lambda)\right]\right\}_+$$

$$+\frac{g_r}{2M_N}\gamma_5\tau_j\frac{(\not p_2+\not q+M_N)}{\nu-\nu_B}\sum_l g_{Tl}t_l\left[T_1^{(l)}(k^2)\sigma^{\lambda\eta}+i\frac{\hat{T}_2^{(l)}(k^2)}{M_N}(\gamma^\lambda k^\eta-\gamma^\eta k^\lambda)\right.$$

$$\left.+\frac{T_3^{(l)}(k^2)}{M_N^2}(\sigma^{\lambda\nu}k_\nu k^\eta-\sigma^{\eta\nu}k_\nu k^\lambda)\right]$$

$$-\sum_l g_{Tl}t_l\left[T_1^{(l)}(k^2)\sigma^{\lambda\eta}+i\frac{\hat{T}_2^{(l)}(k^2)}{M_N}(\gamma^\lambda k^\eta-\gamma^\eta k^\lambda)+\frac{T_3^{(l)}(k^2)}{M_N^2}(\sigma^{\lambda\nu}k_\nu k^\eta-\sigma^{\eta\nu}k_\nu k^\lambda)\right]$$

$$\left.\times\frac{(\not p_1-\not q+M_N)}{\nu+\nu_B}\frac{g_r}{2M_N}\gamma_5\tau_j\right), \tag{19b}$$

$$\mathfrak{M}_j^{T\pi}=\frac{G}{\sqrt{2}}\bar{\nu}\sigma_{\lambda\eta}(1-\gamma_5)\nu\left[g_r\gamma_5\tau_l\frac{1}{(q-k)^2-M_\pi^2}g_{T3}\epsilon^{j13}\frac{T_\pi^{(3)}(k^2)}{M_N}2(q^\lambda k^\eta-q^\eta k^\lambda)\right]. \tag{19c}$$

The term $\mathfrak{M}_j^{T\pi}$ is a pion-pole seagull term describing the tensor-current pion-pole diagram illustrated in Fig. 1(a). Since, as may be seen from Eq. (19c), this term makes a contribution of order q, it is not contained in the basic soft-pion matrix element of Eqs. (19a) and (19b) and so must be added in as a separate contribution. The pion form factor $T_\pi^{(3)}(k^2)$ appearing in Eq. (19c) is defined by[5]

$$\langle\pi^a(p_2)|\mathfrak{F}_3^{\lambda\eta}|\pi^b(p_1)\rangle=\mathfrak{N}_\pi\frac{T_\pi^{(3)}(k^2)}{M_N}\epsilon^{ab3}(P^\lambda k^\eta-P^\eta k^\lambda),$$

$$P=p_1+p_2,\quad k=p_2-p_1, \tag{20}$$

$$\mathfrak{N}_\pi=\frac{1}{(2p_{10}2p_{20})^{1/2}},\quad \epsilon^{123}=1.$$

In addition to the tensor contribution of Fig. 1(a), there is also a scalar-current pion-pole diagram, as illustrated in Fig. 1(b). However, a simple calculation shows that the contribution of this diagram is entirely contained in the commutator term

$$\frac{G}{\sqrt{2}}\bar{\nu}(1-\gamma_5)\nu\left(\frac{-g_r}{M_N g_A}\right)[(\tfrac{2}{3})^{1/2}g_{S0}+(\tfrac{1}{3})^{1/2}g_{S8}] \times t_j F_P^{(3)}((k-q)^2)\gamma_5 \quad (21)$$

appearing in Eq. (21), and so no additional seagull contribution is present in this case.

The procedure for calculating the pion-production cross section is now as follows. First, we use the lepton equations of motion to reduce all induced tensor contributions to an effective scalar-coupling form, via the identity

$$\bar{\nu}(k_2)\sigma_{\lambda\eta}(1-\gamma_5)\nu(k_1)ik^\eta=\bar{\nu}(k_2)(1-\gamma_5)\nu(k_1)(k_1+k_2)_\lambda, \quad (22)$$

and we use Eq. (15) to eliminate factors of γ_5 in the intrinsic tensor contribution via the further identity

$$[\sigma_{\lambda\eta}(1-\gamma_5)]_{ab}[\sigma^{\lambda\eta}\gamma_5]_{cd}=-[\sigma_{\lambda\eta}(1-\gamma_5)]_{ab}[\sigma^{\lambda\eta}]_{cd}. \quad (23)$$

This allows us to write the production matrix element of Eqs. (18)–(19) in terms of a convenient set of 11 basic covariants defined as follows:

$$\mathfrak{M}_\pi=\bar{u}(p_2)(\mathfrak{M}_j^{S,P}+\mathfrak{M}_j^{T}+\mathfrak{M}_j^{T^\pi})u(p_1)\psi_j^*$$

$$=\frac{G}{\sqrt{2}}\bar{\nu}(1-\gamma_5)\nu\,\bar{u}(p_2)\{A_1+\hat{A}_2\gamma_5+A_3\not{q}+C_1(\not{k}_1+\not{k}_2)+C_2[\not{k}_1,\not{k}_2]+C_3[\not{k}_1,\not{k}_2]\gamma_5+\hat{E}_1\not{k}_1\gamma_5+\hat{E}_2\not{k}_2\gamma_5\}u(p_1) \quad (24)$$

$$+\frac{G}{\sqrt{2}}\bar{\nu}\sigma_{\lambda\eta}(1-\gamma_5)\nu\,\bar{u}(p_2)(\hat{B}_1\sigma^{\lambda\eta}+B_3\not{q}\sigma^{\lambda\eta}+B_4\sigma^{\lambda\eta}\not{q})u(p_1).$$

Explicit expressions for the amplitudes $A_1,\ldots,B_4$ are given in Appendix A. From Eq. (24) the pion-production differential cross section may be computed by standard trace techniques, giving the result

$$\frac{d\sigma}{dt\,dW}=\frac{1}{16\pi^3}\frac{|\vec{q}|}{E^2}\frac{G^2}{8M_N^2}\frac{1}{4\pi}\int d\Omega_\pi\Sigma_\pi, \quad (25)$$

with Σ_π being the lengthy expression given in Appendix A. In Eq. (25), W is the invariant mass of the outgoing pion and nucleon, and $|\vec{q}|$ and $d\Omega_\pi=\sin\phi\,d\phi\,d\delta$ are the pion momentum and solid angle in the frame in which the outgoing pion-nucleon isobar is at rest (the isobaric frame). The pion angles ϕ,δ are defined in Ref. 18 and in Fig. 10 below.

Up to this point we have ignored (3,3)-resonance excitation, which can be an important feature of weak-pion production in the S,P,T case if isovector S,P,T couplings are present. A complete treatment of (3,3) excitation requires projecting out the (3,3) multipoles appropriate to the S,P,T case, and then solving the corresponding Omnès equations with the (3,3) projections of Eq. (19) as driving terms. As argued in Sec. IV D of Ref. 18, in cases where the kinematic-singularity-free driving term m^p [obtained by dividing the (3,3) projection of Eq. (19) by the appropriate powers of the isobaric-frame current and pion momenta $|\vec{k}|,|\vec{q}|$] behaves as

$$m^p\approx\frac{\text{const}}{\omega} \quad (26)$$

for small $\omega=W-M_N$, a suitable approximate solution of the Omnès equation for the corresponding kinematic-singularity-free multipole m is

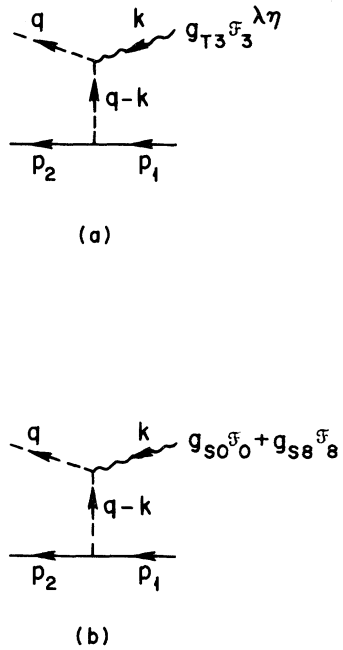

FIG. 1. (a) Tensor-current pion-pole diagram; (b) scalar-current pion-pole diagram. The dashed line denotes the pion, the solid line denotes the nucleon, and the wavy line denotes the external current.

$$m \approx m^D r . \tag{27}$$

Here $r = f_{1+}^{(3/2)}/f_{1+}^{(3/2)B}$ is the ratio of the resonant pion-nucleon partial-wave amplitude to the corresponding Born approximation, which (using the static limit to evaluate $f_{1+}^{(3/2)B}$) is given by[19]

$$r \approx \frac{\exp(i\delta_{3,3})\sin\delta_{3,3}}{|\vec{q}|^3 \tfrac{4}{3} f_r^2/(M_\pi^2\omega)},$$

$$f_r^2 = \frac{1}{4\pi}\left(\frac{M_\pi g_r}{2M_N}\right)^2 \approx 0.080, \tag{28}$$

$$\exp(i\delta_{3,3})\sin\delta_{3,3} = \frac{-\frac{1}{2}\Gamma}{q_0 - q_{0r} + \frac{1}{2}i\Gamma},$$

$$q_{0r} = 1.921 M_\pi,$$

$$\Gamma = (1.262\,|\vec{q}|^3/M_\pi) \times [(q_0 + q_{0r})(1 + 0.504\,|\vec{q}|^2/M_\pi^2)]^{-1}.$$

On the other hand, when the kinematic-singularity–free driving term behaves as

$$m^D \approx \frac{\text{const}}{\omega^2}, \tag{29}$$

the solution to the Omnès equation is approximately

$$m \approx m^D \exp[i\delta_{3,3}]\cos\delta_{3,3}, \tag{30}$$

which vanishes at resonance, although some treatments of pion photoproduction and electroproduction use the resonant solution given in Eq. (27) in this case also.

Application of the above recipe is evidently straightforward, but the work required to do a full multipole analysis in the tensor-coupling case is very considerable. Therefore, as a simple means of getting a preliminary estimate of (3,3)-resonance excitation effects, we have adopted the following procedure. First we evaluate (3,3)-resonance excitation using the static model for pion production,[20] which should give results equivalent to those obtained in leading static approximation by applying the recipe of Eq. (27) to the nucleon-pole-diagram[21] driving terms. In this approximation the scalar amplitude contribution vanishes. To get the leading nonvanishing scalar contribution (and also to get a check on the pure pseudoscalar terms in the static model formula) we treat the scalar and pseudoscalar cases by the multipole expansion method outlined above. The pseudoscalar driving term behaves as in Eq. (26) and, as expected, application of Eq. (27) reproduces the static model result. The scalar driving term behaves as in Eq. (29) and so should presumably be unitarized according to Eq. (30), although we will give numerical results corresponding to the use of Eq. (27) as well. Both the static model and multipole analysis calculations are sketched in Appendix B. Combining the static model and multipole analysis formulas gives an approximate matrix element for resonant pion production in the S,P,T case, which after a straightforward trace calculation and integration over pion angular variables yields the following cross-section formula:

$$\left.\frac{d\sigma}{dt\,dW}\right|_{\text{total}} = \left.\frac{d\sigma}{dt\,dW}\right|_{\text{Eq.(25)}} + \Delta\left(\frac{d\sigma}{dt\,dW}\right), \tag{31}$$

$$\Delta\left(\frac{d\sigma}{dt\,dW}\right) = \frac{G^2}{2\pi^2}\frac{k_{10}k_{20}}{E^2}\left[\frac{2}{9\pi}\frac{g_r^2|\vec{q}|^3}{M_N^2\omega^2}|a_E^{(3/2)}|^2(|r|^2-1)\right]$$
$$\times\left\{\frac{\sin^2(\frac{1}{2}\theta)}{4M_N^2}\left[|g_{P3}F_P^{(3)}(k^2)|^2|\vec{k}|^2 + \frac{16}{M_N^2}k_{10}^2k_{20}^2\sin^2\theta|g_{T3}T_2^{(3)}(k^2)|^2\right]\right.$$
$$+ 4[1+\cos^2(\tfrac{1}{2}\theta)]|g_{T3}T_1^{(3)}(k^2)|^2 + 2\sin^2(\tfrac{1}{2}\theta)\left(\frac{k_{10}+k_{20}}{M_N}\right)\mathrm{Re}[g_{T3}^*T_1^{(3)}(k^2)^*g_{P3}F_P^{(3)}(k^2)]$$
$$\left.+\frac{4k_{10}k_{20}}{M_N^2}\sin^2\theta\,\mathrm{Re}[|g_{T3}|^2T_1^{(3)}(k^2)T_2^{(3)}(k^2)^*]\right\}$$
$$+\frac{G^2}{2\pi^2}\frac{k_{10}k_{20}}{E^2}\left[\frac{2}{9\pi}\frac{g_r^2|\vec{q}|^3}{M_N^2\omega^2}|a_E^{(3/2)}|^2(|s|^2-1)\right]\frac{\sin^2(\frac{1}{2}\theta)}{4M_N^2}\left(\frac{|\vec{q}|\,|\vec{k}|}{\omega}\right)^2|g_{S3}F_S^{(3)}(k^2)|^2.$$

In this equation one has $s = \cos\delta_{3,3}$ if Eq. (30) is used to unitarize the scalar amplitude, while $s = r$ if the Omnès equation for the scalar case is solved as in Eq. (27). The quantities k_{10}, k_{20}, and θ are respectively the isobaric-frame incident neutrino energy, the final neutrino energy, and the neutrino scattering angle, as defined in Sec. II of Ref. 18, where full kinematic details of weak-pion production are given (see also Fig. 10 below). The isospin coefficients $a_E^{(3/2)}$ are tabulated in Table

I. The cross-section addition $\Delta(d\sigma/dt\,dW)$ contains the unitarization factor r in the combination $|r|^2-1$ so as to cancel away the nonunitarized (3,3) multipole contributions coming from the cross section $d\sigma/dt\,dW$ computed in Eq. (25).

Finally, we note that all formulas given in this section have been written assuming incident neutrinos. For incident antineutrinos, all tensor amplitudes are reversed in sign, and in addition the over-all sign of the parity-violating term in Σ_π [the term in Eq. (A5) proportional to $\epsilon_{\alpha\beta\gamma\delta}p_1^\alpha p_2^\beta k_1^\gamma k_2^\delta$] is reversed.[22]

III. NUMERICAL RESULTS

We give in this section sample numerical results obtained from the formulas developed above, as applied to an analysis of low-invariant-mass ($W \leq 1.4$ GeV) pion production in the BNL neutrino flux. Recently, the Columbia-Illinois-Rockefeller collaboration at BNL has reported a measurement of the ratio

$$R_0' = \frac{\sigma(\nu+T\to\nu+\pi^0+\cdots)}{2\sigma(\nu+T\to\mu^-+\pi^0+\cdots)}, \qquad T=\tfrac{1}{4}[{}_6C^{12}]+\tfrac{3}{4}[{}_{13}Al^{27}] \tag{32}$$

with the preliminary result[23]

$$R_0' = 0.17 \pm 0.06. \tag{33}$$

This measured value of R_0' is in accord with the value expected[24] in the Weinberg-Salam model when $\sin^2\theta_W$ is in the currently favored range of 0.3–0.4. Hence *if* (3, 3)-resonance excitation, which is expected in the Weinberg-Salam model, is observed in the BNL experiment, the presumption would be strongly in favor of the standard gauge-theory interpretation of neutral currents. However, preliminary BNL invariant-mass spectra for π^0 production in the charged- and neutral-current cases show a clear (3,3) peak in the charged-current case, but indicate no comparable peaking in the neutral-current reaction. In what follows we analyze the implications for neutral-current structure, in the S, P, T coupling case, if this indication is confirmed both by a more detailed analysis of the BNL data and by other experiments. A similar analysis in the V,A coupling case has been given in Ref. 4.

The simplest (but as we will see below, not the only) interpretation of nonexcitation of the (3,3) resonance would be that the neutral current is pure isoscalar in structure, and we begin our numerical analysis by making this assumption. Applying nuclear charge-exchange corrections as described in Appendix C of Ref. 4, we find that the nuclear target ratio quoted in Eq. (33) implies the free nucleon target ratio

$$2R_0 \equiv \frac{\sigma^{\rm BNL}(\nu+n\to\nu+n+\pi^0)+\sigma^{\rm BNL}(\nu+p\to\nu+p+\pi^0)}{\sigma^{\rm BNL}(\nu+n\to\mu^-+p+\pi^0)} = 2R_0'\times 1.4 = 0.48\pm 0.17, \tag{34}$$

with the superscript BNL denoting averaging of the cross sections over the BNL neutrino flux. Using the theoretical estimate[25]

$$\sigma^{\rm BNL}(\nu+n\to\mu^-+p+\pi^0,\ W\leq 1.4\ {\rm GeV}) \approx 0.14\times 10^{-38}\ {\rm cm}^2, \tag{35}$$

we get from Eq. (34) the cross section for neutral-current π^0 production:

$$\sigma^{\rm BNL}(\nu+n\to\nu+n+\pi^0,\ W\leq 1.4\ {\rm GeV}) + \sigma^{\rm BNL}(\nu+p\to\nu+p+\pi^0,\ W\leq 1.4\ {\rm GeV}) = (68\pm 24)\times 10^{-41}\ {\rm cm}^2, \tag{36}$$

giving one of the basic experimental numbers which must be approximated by the S,P,T fits which we describe below. As we have emphasized in Sec. I, in discussing weak-pion production we will simultaneously take into account the information furnished by experiments studying deep-inelastic neutrino scattering and neutrino-proton elastic scattering. The specific results for these two classes of experiments which we use are the following:

TABLE I. Isospin coefficients appearing in Eq. (31) and in the formulas of Appendixes A and B. The coefficients $a_E^{(I)}$ for definite isospin I are related to $a_E^{(\pm)}$ by $a_E^{(1/2)}=\frac{1}{3}(a_E^{(+)}+a_E^{(-)})$, $a_E^{(3/2)}=\frac{1}{3}(2a_E^{(+)}-a_E^{(-)})$.

Reaction	$a_E^{(+)}$	$a_E^{(-)}$	$a_E^{(0)}$	$a_E^{(1/2)}$	$a_E^{(3/2)}$
$\nu+p\to\nu+p+\pi^0$ $(\bar\nu+p\to\bar\nu+p+\pi^0)$	$\frac{1}{2}$	0	$\frac{1}{2}$	$\frac{1}{6}$	$\frac{1}{3}$
$\nu+n\to\nu+n+\pi^0$ $(\bar\nu+n\to\bar\nu+n+\pi^0)$	$\frac{1}{2}$	0	$-\frac{1}{2}$	$\frac{1}{6}$	$\frac{1}{3}$
$\nu+n\to\nu+p+\pi^-$ $(\bar\nu+n\to\bar\nu+p+\pi^-)$	0	$-\frac{1}{\sqrt{2}}$	$\frac{1}{\sqrt{2}}$	$-\frac{1}{3\sqrt{2}}$	$\frac{1}{3\sqrt{2}}$
$\nu+p\to\nu+n+\pi^+$ $(\bar\nu+p\to\bar\nu+n+\pi^+)$	0	$\frac{1}{\sqrt{2}}$	$\frac{1}{\sqrt{2}}$	$\frac{1}{3\sqrt{2}}$	$-\frac{1}{3\sqrt{2}}$

deep-inelastic neutrino scattering:

(a) $R_\nu = 0.22\pm 0.03$, $R_{\bar\nu} = 0.43\pm 0.12$ (CERN Gargamelle[26]),

$R_\nu = 0.11\pm 0.05$, $R_{\bar\nu} = 0.32\pm 0.09$ [Fermilab Expt. 1A (Ref. 27)],

TABLE II. Central parameter values, parameter variation ranges, and sensitivity to parameter changes of the pion-production cross-section bound implied by Eqs. (37) and (39).

Parameter	$F_S^{(8)}(0)$	$\sigma_{\pi NN}$	$r = F_P^{(0)}(0)/F_P^{(8)}(0)$	$T_1^{(0)}(0)$	$T_1^{(3)}(0)$	$\hat{T}_2^{(0)}(0)$	$\hat{T}_2^{(3)}(0)$	$T_3^{(0)}(0)$	$T_3^{(3)}(0)$	$T_\pi^{(3)}(0)$
Central value [a]	2.95	45 MeV	1	0.87	1.45	−3.75	−0.66	−1.44	0.41	−1.3
Reasonable variation range [b]	1.3 to 4.1	13 to 77 MeV	0.5 to 0.9	$2^{-1/2}\times$ to $2^{1/2}\times$	$2^{-1/2}\times$ to $2^{1/2}\times$	−1× to 2×	−1× to 2×	−1× to 2×	−1× to 2×	$\frac{1}{2}\times$ to 2×
Sensitivity of cross-section bound to parameter variation ($g_{S0}=1$, $g_{T0}=0.4$) [c]										
Varied parameter value	3.72 1.86	15 MeV	... [d]	0.62	2.1	3.75	−1.3	1.44	−0.41	... [d]
Sensitivity ≡ (cross-section bound for varied parameter)/(cross-section bound for central parameters)	0.93 1.15	2.21	...	1.01	1.89	5.3	1.07	1.30	1.11	...

[a] For $F_S^{(8)}(0)$, the value 2.95 is obtained from the quark-model prediction $F_S^{(3)}(0)=0.62$ by using the SU_3 relation $F_S^{(8)}(0)=(3-4\alpha_{SS})F_S^{(3)}(0)$, with $\alpha_{SS}\approx -0.44$; an alternative value of $F_S^{(8)}(0)=1.86$ is obtained from the quark model directly. The quoted value for $\sigma_{\pi NN}$ is the experimental value 45 MeV (±20 MeV) recommended by H. Pilkuhn *et al.* [Nucl. Phys. B65, 460 (1973)]; the quark model value is 28 MeV. All other central values are quark-model values. For the tensor renormalization constants $T_j^{(8)}(0)=T_j^{(0)}(0)$; the remaining scalar and pseudoscalar renormalization constants are given by $F_S^{(3)}(0)=F_S^{(8)}(0)/(3-4\alpha_{SS})$, $F_P^{(3)}(0)=41F_S^{(8)}(0)$, $F_S^{(0)}(0)=F_S^{(8)}(0)\frac{1}{2}[3(\sigma_{\pi NN}/28\text{ MeV})-1]$, $F_P^{(8)}(0)=F_S^{(8)}(0)\times 2.42/(2.66-2.50r)$, $F_P^{(0)}(0)=rF_P^{(8)}(0)$. For further details see Ref. 5.

[b] For $\sigma_{\pi NN}$, the range 13–77 MeV corresponds to the 90% confidence-level limits for the error ±20 MeV quoted by Pilkuhn *et al.* (footnote a above). For the other parameters, the variation ranges are guesses motivated by the discussion of Sec. IV of Ref. 5.

[c] The quoted sensitivities are determined by varying only the indicated parameter, keeping all others fixed at their central values. When all parameters other than $\sigma_{\pi NN}$ are given the indicated varied values and then stepped back one at a time to the central values, sensitivities approximately consistent with those in the table are obtained.

[d] For the SU_3-singlet scalar-tensor mixture assumed in the sensitivity study, the cross-section bound is independent of the parameter r and $T_\pi^{(3)}(0)$.

$R_\nu = 0.22$, $R_{\bar\nu} = 0.33$ (Caltech-Fermilab raw data[28]),

$\Rightarrow 3R_\nu + R_{\bar\nu} \leq 1.5$ at 95% confidence level, (37)

(b) y distribution inconsistent with y^2, consistent with somewhere between $V-A$ and $V+A$, with T or with T, S, P mixtures (Caltech-Fermilab[29]);

neutrino-proton elastic scattering:

$$\sigma^{\rm CERN}(\nu+p\to\nu+p,\ \text{Cundy cuts}) \leq 0.24\,\sigma^{\rm CERN}(\nu+n\to\mu^-+p,\ \text{Cundy cuts}) \quad (38)$$

at 95% confidence level; Cundy[30] cuts are

$1 \leq E \leq 4$ GeV, $0.3 \leq |k^2| \leq 1$ (GeV/c)^2.

Neglecting possible distorting effects of the cuts, and using the fact that the CERN and BNL neutrino fluxes are similar[31] in shape, Eq. (38) gives an approximate bound for the BNL flux-averaged neutrino-proton elastic cross section,

$$\sigma^{\rm BNL}(\nu+p\to\nu+p) \lesssim 0.24\,\sigma^{\rm BNL}(\nu+n\to\mu^-+p) = 0.21\times10^{-38}\ \text{cm}^2$$

at 95% confidence level. (39)

As is evident from the formulas of Sec. II, the S, P, T cross sections involve many coupling constants and form factors (the pion-production cross sections depend on 21 independent form factor combinations in all) and so adoption of a fairly systematic procedure for searching for fits is essential. The procedure which we have used is as follows[32]:

(1) In studying the isoscalar case we make the further simplifying restriction to purely unitary singlet weak neutral couplings. Hence we take

$$g_{S3}=g_{S8}=0,\quad g_{P3}=g_{P8}=0,\quad g_{T3}=g_{T8}=0, \quad (40)$$

so that the quark structure of the weak neutral interaction is completely specified by the three coupling parameters g_{S0}, g_{P0}, g_{T0}.

(2) We follow the conventional practice of parameterizing nucleon form factors in dipole form and meson form factors in monopole form. Hence for all S, P, T form factors not connected with pion exchange we use the parameterization

$$F(k^2) = F(0)(1-k^2/M^2)^{-2}, \quad (41a)$$

while the form factors $T_\pi^{(3)}(k^2)$ and $F_P^{(3)}(k^2)$ are parameterized as

$$T_\pi^{(3)}(k^2) = T_\pi^{(3)}(0)(1-k^2/M^2)^{-1},$$
$$F_P^{(3)}(k^2) = F_P^{(3)}(0)(1-k^2/M_\pi^2)^{-1}(1-k^2/M^2)^{-1}. \quad (41b)$$

For the form-factor mass M we take the value

$$M \approx 0.9\ \text{GeV} \quad (41c)$$

suggested by quark-model[5,33] considerations.

(3) For the form-factor values at $k^2=0$ (i.e., for

TABLE III. Parameter values for fits Nos. 1–5.

	Fit No. 1	Fit No. 2	Fit No. 3	Fit No. 4	Fit No. 5
g_{S0}	$1\times f$	0	$0.5\times f$	$1\times f$	$1\times f$
g_{P0}	0	$1\times f$	$-0.5\times f$	0	0
g_{T0}	$-0.4\times f$	$0.4\times f$	$-0.25\times f$	$-0.4\times f$	$-0.25\times f$
f	1.12	1.10	1.92	1.17	1.47
$F_S^{(8)}(0)$	3.72	3.72	3.72	1.86	3.72
$\sigma_{\pi NN}$	45 MeV	···	45 MeV.	45 MeV	28 MeV
r	···	0.7	0.7	···	···
$T_1^{(0)}(0)$	0.62	0.62	0.62	0.62	0.62
$T_1^{(3)}(0)$	2.1	2.1	2.1	2.1	2.1
$\hat T_2^{(0)}(0)$	−0.75	−0.75	−0.75	−0.75	1.9
$\hat T_2^{(3)}(0)$	−1.3	−1.3	−1.3	−1.3	−1.9
$T_3^{(0)}(0)$	−0.72	−0.72	−0.72	−0.72	0.66
$T_3^{(3)}(0)$	0.2	0.2	0.2	0.2	−0.3

the S,P,T renormalization parameters analogous to the V,A renormalization constants g_A, μ^V, etc.) we start from central values suggested by the analysis of Ref. 5, which we have tabulated on the first line of Table II. A numerical survey (using an interactive time-sharing facility) indicates that these parameter values do not give satisfactory fits for the various coupling patterns of interest, such as a pure tensor weak neutral interaction or scalar-tensor or pseudoscalar-tensor mixtures. Instead, we find with the central parameter values that when the deep-inelastic and elastic scattering constraints of Eqs. (37) and (39) are imposed, the resulting bound[34] on the pion-production cross section $\sigma^{\mathrm{BNL}}(\nu n\pi^0+\nu p\pi^0,\ W\leq 1.4\ \mathrm{GeV})$ is typically a factor of 3 or more smaller than the experimental value of Eq. (36).

(4) We next permit reasonable variations of the parameters from the central values, as shown in the second line of Table II, making possible increases in the bound on the pion-production cross section imposed by Eqs. (37) and (39). The sensitivity of the pion production bound to parameter changes (for a scalar-tensor mixture) is indicated in the bottom two lines of Table II. Evidently, the bound is most sensitive to changes in $\hat{T}_2^{(0)}(0)$, $T_1^{(3)}(0)$ and $\sigma_{\pi NN}$, and relatively less sensitive to variations in the other parameters. If the parameter $T_1^{(3)}(0)$ is increased without limit, the cross-section bound approaches infinity, as a result of the fact that the pion-production cross section receives a contribution from $T_1^{(3)}(0)$ via the equal-time commutator term in Eq. (12), whereas (in the SU(3)-singlet current case) the elastic neutrino-proton cross section is independent of $T_1^{(3)}(0)$. This is of course a consequence of the SU(3) D-type

TABLE IV. Values of physical quantities in fits Nos. 1–5.

	Fit No. 1	Fit No. 2	Fit No. 3	Fit No. 4	Fit No. 5
Limiting inequality [a]	Elastic scattering Eq. (39)	Deep inelastic Eq. (37)	Elastic scattering Eq. (39)	Deep inelastic Eq. (37)	Deep inelastic Eq. (37)
$\sigma^{\mathrm{BNL}}(\nu p)$ [b] in 10^{-38} cm^2	0.18	0.058	0.18	0.094	0.027
$\sigma^{\mathrm{BNL}}(\bar{\nu}p)$ in 10^{-38} cm^2	0.080	0.032	0.058	0.032	0.19
R_ν	0.23	0.22	0.31	0.25	0.20
$R_{\bar{\nu}}$	0.35	0.34	0.31	0.38	0.23
$\sigma^{\mathrm{BNL}}(\nu n\pi^0+\nu p\pi^0,\ W\leq 1.4\ \mathrm{GeV})$ in 10^{-41} cm^2	62	56	73	61	68
$\sigma^{\mathrm{BNL}}(\bar{\nu}n\pi^0+\bar{\nu}p\pi^0,\ W\leq 1.4\ \mathrm{GeV})$ in 10^{-41} cm^2	48	49	55	51	38
$\sigma_{2\ \mathrm{bin}}^{\mathrm{ANL}}(\nu p\pi^-)$ in 10^{-41} cm^2	2.7	1.8	3.0	2.3	3.6
$\sigma^{\mathrm{ANL}}(\nu p\pi^-,\ W\leq 1.4\ \mathrm{GeV})$ in 10^{-41} cm^2	32	25	37	28	40
$a_0{}^2$ [c]	22	0	16	6	10
$\sigma^{\mathrm{ANL}}(\nu p)$ in 10^{-38} cm^2	0.34	0.057	0.30	0.13	0.079
$\sigma(\nu p)$ at $E=50$ MeV in 10^{-39} cm^2	0.37	0.0082	0.28	0.11	0.16

[a] By limiting inequality we mean which of the two inequalities, Eq. (37) or Eq. (39), is saturated first when the overall strength of the weak neutral interaction is scaled up.

[b] The superscripts BNL, ANL denote cross sections averaged over the Brookhaven National Laboratory and the Argonne National Laboratory neutrino flux distributions, respectively. The quantity $\sigma_{2\ \mathrm{bin}}^{\mathrm{ANL}}$ is defined in Ref. 4.

[c] The coherent neutrino scattering parameter $a_0{}^2$ was introduced by Freedman [D. Z. Freedman, Phys. Rev. D 9, 1389 (1974)] by writing the neutrino-nucleus coherent cross section, in the vector case, in the form $d\sigma^{V,\mathrm{coh}}/dz = [E^2G^2A^2/(2\pi)]a_0{}^2(1+z)$, with A being the atomic weight and z being the cosine of the neutrino scattering angle. In the scalar case we define $a_0{}^2$ by writing $d\sigma^{S,\mathrm{coh}}/dz = [E^2G^2A^2/(2\pi)]\frac{1}{2}a_0{}^2(1-z)$, with the additional factor of $\frac{1}{2}$ reflecting the fact that a $(1-z)$ angular distribution produces twice the radiation pressure of a $(1+z)$ angular distribution [see S. L. Adler, Phys. Rev. D 11, 1155 (1975)]. From the formulas of Sec. II2A, we thus find in the scalar case that $a_0{}^2 = 2F_S^T(0)^2$.

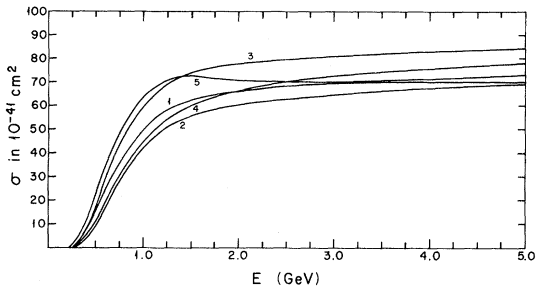

FIG. 2. Cross section $\sigma(\nu+n\to\nu+n+\pi^0)$ $+\sigma(\nu+p\to\nu+p+\pi^0)$ versus incident neutrino energy E for fits Nos. 1–5.

commutator structure in the S,P,T case, which permits $[F_j^S, \mathcal{J}(0)]$ to lie in a different isospin multiplet from the current $\mathcal{J}(0)$ itself. Hence, in the S,P,T isoscalar case there is no analog to the parameter-independent bounds on the pion-production cross section which are found[4] in the V,A isoscalar case.

Allowing the renormalization parameters to vary within the ranges indicated in Table II, we have constructed a series of fits to the experimental data summarized in Eqs. (36)–(39) above. The features of five representative fits, with rather different characteristics, are given in Tables III and IV and Figs. 2–7. The parameters of the fits are summarized in Table III; fit No. 1 is a scalar-tensor fit with large scalar renormalization parameters; fit No. 2 is a pseudoscalar-tensor fit; fit No. 3 is a scalar-pseudoscalar-tensor mixture which, like the combination $V-A$, is a formal Fierz transformation[35] invariant; fit No. 4 is a scalar-tensor mixture with reduced scalar renormalization parameters; while fit No. 5 is a scalar-tensor fit with $\hat{T}_2^{(0)}$ reversed in sign from its central value. Some physical quantites of interest in the various fits are tabulated in Table IV. In Figs. 2 and 3 we give neutrino- and antineutrino-induced pion-production cross sections for the

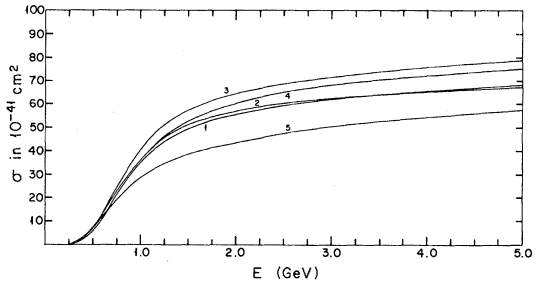

FIG. 3. Cross section $\sigma(\bar{\nu}+n\to\bar{\nu}+n+\pi^0)$ $+\sigma(\bar{\nu}+p\to\bar{\nu}+p+\pi^0)$ versus incident antineutrino energy E for fits Nos. 1–5.

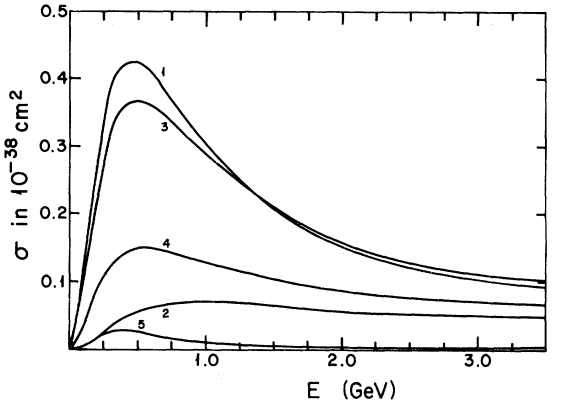

FIG. 4. Cross section $\sigma(\nu+p\to\nu+p)$ versus incident neutrino energy E for fits Nos. 1–5.

various fits; the curves are evidently all qualitatively quite similar. On the other hand, the neutrino-proton and antineutrino-proton elastic cross sections illustrated in Figs. 4 and 5 differ widely between the fits. One interesting feature of fit No. 5 is that although the scalar-tensor interference is constructive in neutrino pion production, giving $\sigma(\nu n\pi^0+\nu p\pi^0)>\sigma(\bar{\nu}n\pi^0+\bar{\nu}p\pi^0)$, it is strongly destructive in neutrino-proton elastic scattering, so that $\sigma(\nu p)\ll\sigma(\bar{\nu}p)$. This sign reversal in the interference terms is absent in fits Nos. 1–4, where both the neutrino-induced pion production and elastic cross sections are larger than their antineutrino-induced counterparts. In Figs. 6 and 7 we have plotted the deep-inelastic y distributions for the various fits, together, for comparison, with the y distribution expected[10] in the Weinberg-Salam model for $\sin^2\theta_W=0.35$. The close similarity of the various curves, in both the incident neutrino and the incident antineutrino cases, is evident. One obvious qualitative feature of all of the

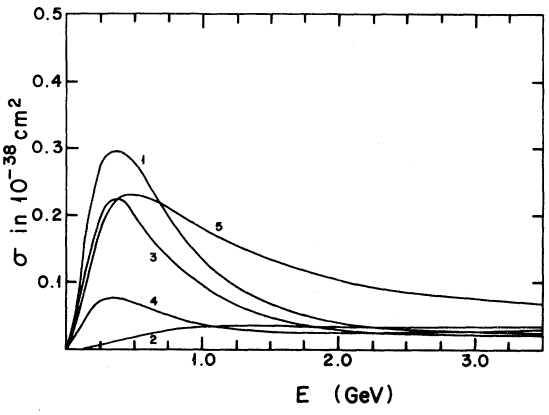

FIG. 5. Cross section $\sigma(\bar{\nu}+p\to\bar{\nu}+p)$ versus incident antineutrino energy E for fits Nos. 1–5.

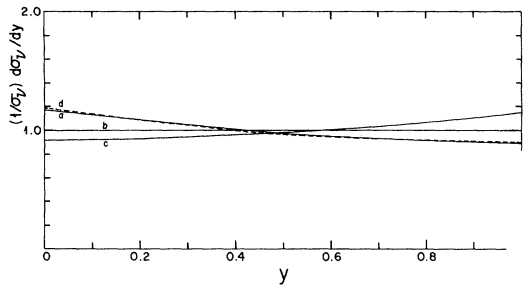

FIG. 6. Unit-normalized deep-inelastic y distributions for incident neutrinos. Curve a: fits Nos. 1, 2, and 4; curve b: fit No. 3, curve c: fit No. 5. The y distribution for the Weinberg-Salam model with $\sin^2\theta_W = 0.35$ is shown in curve d.

fits is that since both even (S and/or P) and odd (T) charge conjugation pieces are present in the weak neutral interaction, neutrino and antineutrino cross sections differ. However, since a CP-conserving S,P,T Lagrangian is still parity-conserving, the presence of (S,P)-T mixtures does not imply parity-violating effects in processes in which neutrinos are not involved, such as the pp, ep, and μp interactions.[36] By contrast, in the V,A coupling case[4] the presence of neutrino-antineutrino cross-section differences is in general accompanied by parity-violating neutral-current effects in non-neutrino-induced reactions.

Up to this point we have restricted the discussion to purely isoscalar (in fact, purely SU_3 singlet) S,P,T neutral couplings. In order to study the effect of isovector admixtures, we have considered modifications of fits Nos. 1 or 2 obtained by allowing either g_{S3}, g_{P3} or g_{T3} to be nonzero, as detailed in Table V. The resulting $d\sigma^{\rm BNL}/dW$ distributions are graphed in Fig. 8. The qualitative conclusion which emerges from this study is that isovector tensor or pseudoscalar couplings lead to strong (3,3) peaking in invariant-mass plots, but an isovector scalar component can be present without producing a visible (3,3) peak, even when it produces strong deviations of the final πN charge-state ratios from the values which they have in the isoscalar case.[37] Hence a nonresonant invariant-mass plot does not in itself imply an isoscalar neutral interaction in the S,P,T case; branching-ratio information is also needed to exclude an isovector scalar component.

As we have already emphasized, the S,P,T cross sections involve a large number of parameters and this fact, together with the scanty experimental information presently available, does not permit any definite conclusions about the presence or absence of S,P,T neutral interactions to be made at this time. Looking ahead, we have written general and flexible computer programs embodying the calculations of this paper, along with corresponding programs for the general V,A neutral-current case.[4,6] As improved experimental data becomes available, these programs will be used to give updated, and hopefully more restrictive, analyses of the phenomenological form of the weak neutral coupling.

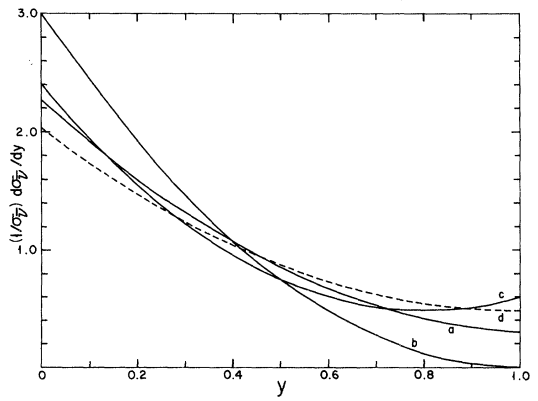

FIG. 7. Unit-normalized deep-inelastic y distributions for incident antineutrinos. Curve a: fits Nos. 1, 2, and 4; curve b: fit No. 3; curve c: fit No. 5. The y distribution for the Weinberg-Salam model with $\sin^2\theta_W = 0.35$ is shown in curve d.

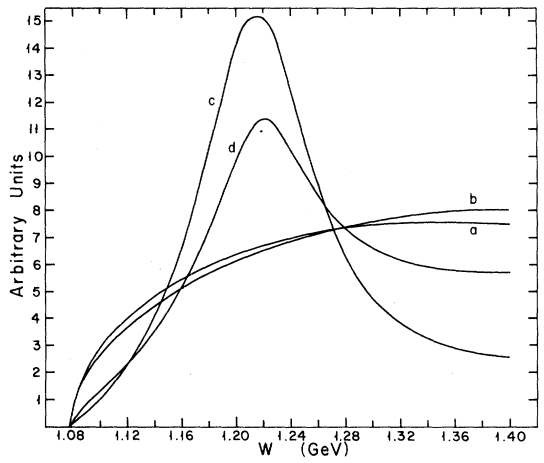

FIG. 8. Curves giving $d\sigma/dW$ for the reaction $\nu + p \to \nu + p + \pi^0$, averaged over the BNL neutrino flux. Curve a: fit No. 1; curve b: fit No. 1 with $g_{S3} = 6^{1/2}$ [the two methods of treating the resonant scalar multipole described following Eq. (31) give virtually the same curve]; curve c: fit No. 1 with $g_{T3} = -0.4 \times 6^{1/2}$; curve d: fit No. 2 with $g_{P3} = 6^{1/2}$. The four curves have been normalized to equal area. Curve a is typical of the normalized $d\sigma^{\rm BNL}/dW$ distribution for all of the isoscalar fits considered, and in effect represents BNL phase space for the pion-production process.

TABLE V. Relative isoscalar cross sections together with cross sections for three modified fits with isovector additions to the S, T, and P parts, respectively.

Parameters [a]	$\nu+p\to\nu+p+\pi^0$	$\nu+n\to\nu+n+\pi^0$	$\nu+n\to\nu+p+\pi^-$	$\nu+p\to\nu+n+\pi^+$
Isoscalar case cross sections (arbitrary units)	1	1	2	2
Fit No. 1 with [b] $g_{S3}=6^{1/2}$	68	32	61	70
Fit No. 1 with $g_{T3}=-0.4\times 6^{1/2}$	78	71	57	77
Fit No. 2 with $g_{P3}=6^{1/2}$	29	20	19	15

[a] The isovector additions used would make the scalar, pseudoscalar, and tensor currents, respectively, U-spin singlets in the limit in which $F_S^{(0)}=F_S^{(8)}$, $F_P^{(0)}=F_P^{(8)}$, and $T_j^{(0)}=T_j^{(8)}$, $j=1,2,3$. For the actual renormalization-constant values used in fits Nos. 1 and 2, the isovector tensor case given in the table corresponds to a tensor U-spin singlet structure, the isovector pseudoscalar addition is smaller (by a factor of $r=0.7$) than is required to make a pseudoscalar U-spin singlet, while the isovector scalar addition is larger (by a factor of 1.9) than is required to make a scalar U-spin singlet.

[b] The cross sections in this case are virtually independent of whether the scalar enhancement factor s of Eq. (31) is taken as $\cos\delta_{(3,3)}$ or as r.

ACKNOWLEDGMENTS

We wish to thank R. Palais for assistance in setting up the time-sharing part of the computer work, S. B. Treiman for many helpful comments in the course of this work, and members of the Columbia-Illinois-Rockefeller collaboration for conversations about the BNL pion-production experiment.

APPENDIX A: FORMULAS FOR PION-PRODUCTION AMPLITUDES AND CROSS SECTION

In this appendix we give the expressions for the 11 amplitudes $A_1,\ldots,B_4$ which parameterize the pion-production amplitude [Eq. (24)] and for the resulting matrix element squared Σ_π which occurs in the cross section [Eq. (25)]. The expressions which follow involve the isospin matrix elements

$$a_E^{(\pm)}=\chi_2^\dagger\psi_j^{*}\tfrac{1}{4}(\tau_j\tau_3\pm\tau_3\tau_j)\chi_1\,,$$
$$a_E^{(0)}=\chi_2^\dagger\psi_j^{*}\tfrac{1}{2}\tau_j\chi_1\,, \qquad \text{(A1)}$$

where $\chi_{1,2}$ are the initial and final nucleon isospinors and ψ_j is the final pion isospin wave function. Their numerical values for different channels are given in Table I.

We write the matrix element in the form

$$\mathfrak{M}_\pi=\frac{G}{\sqrt{2}}\,\bar\nu(1-\gamma_5)\nu\bar u(p_2)\{A_1+A_2\gamma_5+A_3\not q+A_4\not q\gamma_5+C_1(\not k_1+\not k_2)+C_2[\not k_1,\not k_2]+C_3[\not k_1,\not k_2]\gamma_5+E_1\not k_1\gamma_5+E_2\not k_2\gamma_5\}u(p_1)$$
$$+\frac{G}{\sqrt{2}}\,\bar\nu\sigma_{\lambda\eta}(1-\gamma_5)\nu\bar u(p_2)(B_1\sigma^{\lambda\eta}+B_2\sigma^{\lambda\eta}\gamma_5+B_3\gamma_5\not q\sigma^{\lambda\eta}+B_4\sigma^{\lambda\eta}\not q\gamma_5)u(p_1)\,. \qquad \text{(A2)}$$

The amplitudes in this expression are related to the amplitudes defined in Eq. (24) by

$$\hat A_2=A_2-2M_NA_4\,,$$
$$\hat E_1=E_1+A_4\,,$$
$$\hat E_2=E_2-A_4\,, \qquad \text{(A3)}$$
$$\hat B_1=B_1-B_2\,,$$

$$A_1=-\frac{g_r}{M_Ng_A}\{[(\tfrac{2}{3})^{1/2}g_{P0}+(\tfrac{1}{3})^{1/2}g_{P8}]a_E^{(0)}F_S^{(3)}(k^2)+g_{P3}a_E^{(+)}[\tfrac{2}{3}F_S^{(0)}(k^2)+\tfrac{1}{3}F_S^{(8)}(k^2)]\}$$
$$+\frac{g_r}{2M_N}\{2a_E^{(0)}[(\tfrac{2}{3})^{1/2}g_{P0}F_P^{(0)}(k^2)+(\tfrac{1}{3})^{1/2}g_{P8}F_P^{(8)}(k^2)]+2a_E^{(+)}g_{P3}F_P^{(3)}(k^2)\}\,,$$

$$A_2 = -\frac{g_r}{M_N g_A}\{[(\tfrac{2}{3})^{1/2} g_{S0} + (\tfrac{1}{3})^{1/2} g_{S8}]\, a_E^{(0)} F_P^{(3)}((k-q)^2) + g_{S3} a_E^{(+)}[\tfrac{2}{3}F_P^{(0)}(k^2) + \tfrac{1}{3}F_P^{(8)}(k^2)]\}$$
$$+ \frac{g_r}{2M_N}\{2a_E^{(0)}[(\tfrac{2}{3})^{1/2} g_{S0} F_S^{(0)}(k^2) + (\tfrac{1}{3})^{1/2} g_{S8} F_S^{(8)}(k^2)] + 2a_E^{(+)} g_{S3} F_S^{(3)}(k^2)\} + g_r \frac{1}{(q-k)^2 - M_\pi^2} g_{T3}\, 2a_E^{(-)} \frac{T_\pi^{(3)}(k^2)}{M_N}\, 4q\cdot K$$
$$+ \frac{g_r}{2M_N}\frac{1}{\nu-\nu_B}\left\{a_E^{(0)}\left[(\tfrac{2}{3})^{1/2} g_{T0}\frac{2\hat{T}_2^{(0)}(k^2)}{M_N} + (\tfrac{1}{3})^{1/2} g_{T8}\frac{2\hat{T}_2^{(8)}(k^2)}{M_N}\right] + (a_E^{(+)} + a_E^{(-)}) g_{T3}\frac{2\hat{T}_2^{(3)}(k^2)}{M_N}\right\} 2p_1\cdot K$$
$$- 2p_2\cdot K\left\{a_E^{(0)}\left[(\tfrac{2}{3})^{1/2} g_{T0}\frac{2\hat{T}_2^{(0)}(k^2)}{M_N} + (\tfrac{1}{3})^{1/2} g_{T8}\frac{2\hat{T}_2^{(8)}(k^2)}{M_N}\right] + (a_E^{(+)} - a_E^{(-)}) g_{T3}\frac{2\hat{T}_2^{(3)}(k^2)}{M_N}\right\}\frac{1}{\nu+\nu_B}\frac{g_r}{2M_N},$$

$$A_3 = -\frac{g_r}{2M_N}\frac{1}{\nu-\nu_B}\{a_E^{(0)}[(\tfrac{2}{3})^{1/2} g_{P0} F_P^{(0)}(k^2) + (\tfrac{1}{3})^{1/2} g_{P8} F_P^{(8)}(k^2)] + (a_E^{(+)} + a_E^{(-)}) g_{P3} F_P^{(3)}(k^2)\}$$
$$- \{a_E^{(0)}[(\tfrac{2}{3})^{1/2} g_{P0} F_P^{(0)}(k^2) + (\tfrac{1}{3})^{1/2} g_{P8} F_P^{(8)}(k^2)] + (a_E^{(+)} - a_E^{(-)}) g_{P3} F_P^{(3)}(k^2)\}\frac{1}{\nu+\nu_B}\frac{g_r}{2M_N},$$

$$A_4 = -\frac{g_r}{2M_N}\frac{1}{\nu-\nu_B}\{a_E^{(0)}[(\tfrac{2}{3})^{1/2} g_{S0} F_S^{(0)}(k^2) + (\tfrac{1}{3})^{1/2} g_{S8} F_S^{(8)}(k^2)] + (a_E^{(+)} + a_E^{(-)}) g_{S3} F_S^{(3)}(k^2)\}$$
$$+ \{a_E^{(0)}[(\tfrac{2}{3})^{1/2} g_{S0} F_S^{(0)}(k^2) + (\tfrac{1}{3})^{1/2} g_{S8} F_S^{(8)}(k^2)] + (a_E^{(+)} - a_E^{(-)}) g_{S3} F_S^{(3)}(k^2)\}\frac{1}{\nu+\nu_B}\frac{g_r}{2M_N},$$

$$C_1 = \frac{g_r}{M_N g_A}\left\{a_E^{(0)}[(\tfrac{2}{3})^{1/2} g_{T0} + (\tfrac{1}{3})^{1/2} g_{T8}]\frac{2\hat{T}_2^{(3)}(k^2)}{M_N} + \frac{2}{M_N} g_{T3} a_E^{(+)}[\tfrac{2}{3}\hat{T}_2^{(0)}(k^2) + \tfrac{1}{3}\hat{T}_2^{(8)}(k^2)]\right\},$$

$$C_2 = -\frac{g_r}{M_N g_A}\left\{a_E^{(0)}[(\tfrac{2}{3})^{1/2} g_{T0} + (\tfrac{1}{3})^{1/2} g_{T8}]\frac{2T_3^{(3)}(k^2)}{M_N^2} + \frac{2}{M_N^2} g_{T3} a_E^{(+)}[\tfrac{2}{3}T_3^{(0)}(k^2) + \tfrac{1}{3}T_3^{(8)}(k^2)]\right\},$$

$$C_3 = -\frac{g_r}{2M_N}\left\{2a_E^{(0)}\left[(\tfrac{2}{3})^{1/2} g_{T0}\frac{2T_3^{(0)}(k^2)}{M_N^2} + (\tfrac{1}{3})^{1/2} g_{T8}\frac{2T_3^{(8)}(k^2)}{M_N^2}\right] + 2a_E^{(+)} g_{T3}\frac{2T_3^{(3)}(k^2)}{M_N^2}\right\}$$
$$+ \frac{g_r}{2M_N}\frac{1}{\nu-\nu_B}\left\{a_E^{(0)}\left[(\tfrac{2}{3})^{1/2} g_{T0}\frac{2T_2^{(0)}(k^2)}{M_N} + (\tfrac{1}{3})^{1/2} g_{T8}\frac{2T_2^{(8)}(k^2)}{M_N}\right] + (a_E^{(+)} + a_E^{(-)}) g_{T3}\frac{2T_2^{(3)}(k^2)}{M_N}\right\}$$
$$- \left\{a_E^{(0)}\left[(\tfrac{2}{3})^{1/2} g_{T0}\frac{2T_2^{(0)}(k^2)}{M_N} + (\tfrac{1}{3})^{1/2} g_{T8}\frac{2T_2^{(8)}(k^2)}{M_N}\right] + (a_E^{(+)} - a_E^{(-)}) g_{T3}\frac{2T_2^{(3)}(k^2)}{M_N}\right\}\frac{1}{\nu+\nu_B}\frac{g_r}{2M_N}, \tag{A4}$$

$$E_1 = -\frac{g_r}{2M_N} g_{T3}\, 2a_E^{(-)}\frac{2\hat{T}_2^{(3)}(k^2)}{M_N}$$
$$+ \frac{g_r}{2M_N}\frac{1}{\nu-\nu_B}\left\{a_E^{(0)}\left[(\tfrac{2}{3})^{1/2} g_{T0}\frac{2T_3^{(0)}(k^2)}{M_N^2} + (\tfrac{1}{3})^{1/2} g_{T8}\frac{2T_3^{(8)}(k^2)}{M_N^2}\right] + (a_E^{(+)} + a_E^{(-)}) g_{T3}\frac{2T_3^{(3)}(k^2)}{M_N^2}\right\}(-2k_1\cdot k_2 - 4p_1\cdot k_2)$$
$$+ (-2k_1\cdot k_2 + 4p_2\cdot k_2)\left\{a_E^{(0)}\left[(\tfrac{2}{3})^{1/2} g_{T0}\frac{2T_3^{(0)}(k^2)}{M_N^2} + (\tfrac{1}{3})^{1/2} g_{T8}\frac{2T_3^{(8)}(k^2)}{M_N^2}\right] + (a_E^{(+)} - a_E^{(-)}) g_{T3}\frac{2T_3^{(3)}(k^2)}{M_N^2}\right\}\frac{1}{\nu+\nu_B}\frac{g_r}{2M_N},$$

$$E_2 = -\frac{g_r}{2M_N} g_{T3}\, 2a_E^{(-)}\frac{2\hat{T}_2^{(3)}(k^2)}{M_N}$$
$$+ \frac{g_r}{2M_N}\frac{1}{\nu-\nu_B}\left\{a_E^{(0)}\left[(\tfrac{2}{3})^{1/2} g_{T0}\frac{2T_3^{(0)}(k^2)}{M_N^2} + (\tfrac{1}{3})^{1/2} g_{T8}\frac{2T_3^{(8)}(k^2)}{M_N^2}\right] + (a_E^{(+)} + a_E^{(-)}) g_{T3}\frac{2T_3^{(3)}(k^2)}{M_N^2}\right\}(-2k_1\cdot k_2 + 4p_1\cdot k_1)$$
$$+ (-2k_1\cdot k_2 - 4p_2\circ k_1)\left\{a_E^{(0)}\left[(\tfrac{2}{3})^{1/2} g_{T0}\frac{2T_3^{(0)}(k^2)}{M_N^2} + (\tfrac{1}{3})^{1/2} g_{T8}\frac{2T_3^{(8)}(k^2)}{M_N^2}\right] + (a_E^{(+)} - a_E^{(-)}) g_{T3}\frac{2T_3^{(3)}(k^2)}{M_N^2}\right\}\frac{1}{\nu+\nu_B}\frac{g_r}{2M_N},$$

$$B_1 = \frac{g_r}{M_N g_A}\{a_E^{(0)}[(\tfrac{2}{3})^{1/2} g_{T0} + (\tfrac{1}{3})^{1/2} g_{T8}]\, T_1^{(3)}(k^2) + a_E^{(+)} g_{T3}[\tfrac{2}{3}T_1^{(0)}(k^2) + \tfrac{1}{3}T_1^{(8)}(k^2)]\},$$

$$B_2 = \frac{g_r}{2M_N}\{2a_E^{(0)}[(\tfrac{2}{3})^{1/2} g_{T0} T_1^{(0)}(k^2) + (\tfrac{1}{3})^{1/2} g_{T8} T_1^{(8)}(k^2)] + 2a_E^{(+)} g_{T3} T_1^{(3)}(k^2)\},$$

$$B_3 = \frac{g_r}{2M_N}\frac{1}{\nu-\nu_B}\{a_E^{(0)}[(\tfrac{2}{3})^{1/2} g_{T0} T_1^{(0)}(k^2) + (\tfrac{1}{3})^{1/2} g_{T8} T_1^{(8)}(k^2)] + (a_E^{(+)} + a_E^{(-)}) g_{T3} T_1^{(3)}(k^2)\},$$

$$B_4 = \{a_E^{(0)}[(\tfrac{2}{3})^{1/2} g_{T0} T_1^{(0)}(k^2) + (\tfrac{1}{3})^{1/2} g_{T8} T_1^{(8)}(k^2)] + (a_E^{(+)} - a_E^{(-)}) g_{T3}\, T_1^{(3)}(k^2)\}\frac{1}{\nu+\nu_B}\frac{g_r}{2M_N}.$$

Taking the traces, we find

$$
\begin{aligned}
\Sigma_\pi = \frac{8M_N{}^2 m_\nu{}^2}{G^2}\langle|\mathfrak{M}_\pi|^2\rangle
&= k_1\cdot k_2\{4|A_1|^2(p_1\cdot p_2+M_N{}^2)+4|\hat{A}_2|^2(p_1\cdot p_2-M_N{}^2)+4|A_3|^2[2p_1\cdot qp_2\cdot q-q^2(p_1\cdot p_2-M_N{}^2)]\\
&\quad+4|C_1|^2[2p_1\cdot Kp_2\cdot K-K^2(p_1\cdot p_2-M_N{}^2)]\\
&\quad+16|C_2|^2[-(k_1\cdot k_2)^2(p_1\cdot p_2+M_N{}^2)+2k_1\cdot k_2k_1\cdot p_1k_2\cdot p_2+2k_1\cdot k_2k_1\cdot p_2k_2\cdot p_1]\\
&\quad+16|C_3|^2[-(k_1\cdot k_2)^2(p_1\cdot p_2-M_N{}^2)+2k_1\cdot k_2k_1\cdot p_1k_2\cdot p_2+2k_1\cdot k_2k_1\cdot p_2k_2\cdot p_1]\\
&\quad+8|\hat{E}_1|^2p_1\cdot k_1p_2\cdot k_1+8|\hat{E}_2|^2p_1\cdot k_2p_2\cdot k_2+8M_N\mathrm{Re}(A_1^*A_3)q\cdot(p_1+p_2)+8M_N\mathrm{Re}(A_1^*C_1)K\cdot(p_1+p_2)\\
&\quad+16\,\mathrm{Re}(A_1^*C_2)(p_1\cdot k_2p_2\cdot k_1-p_1\cdot k_1p_2\cdot k_2)+16\,\mathrm{Re}(\hat{A}_2^*C_3)(p_1\cdot k_2p_2\cdot k_1-p_1\cdot k_1p_2\cdot k_2)\\
&\quad-8\,\mathrm{Re}(\hat{A}_2^*\hat{E}_1)M_Nk_1\cdot(p_2-p_1)-8\,\mathrm{Re}(\hat{A}_2^*\hat{E}_2)M_Nk_2\cdot(p_2-p_1)\\
&\quad+8\,\mathrm{Re}(A_3^*C_1)[p_1\cdot qp_2\cdot K+p_1\cdot Kp_2\cdot q-q\circ K(p_1\cdot p_2-M_N{}^2)]\\
&\quad+16\,\mathrm{Re}(A_3^*C_2)M_N[q\cdot k_1k_2\cdot(p_1-p_2)-q\cdot k_2k_1\cdot(p_1-p_2)]+16\,\mathrm{Re}(C_1^*C_2)M_Nk_1\cdot k_2(p_1-p_2)\cdot(k_2-k_1)\\
&\quad-16\,\mathrm{Re}(C_3^*\hat{E}_1)M_Nk_1\cdot k_2k_1\cdot(p_1+p_2)+16\,\mathrm{Re}(C_3^*\hat{E}_2)M_Nk_1\cdot k_2k_2\cdot(p_1+p_2)\\
&\quad+8\,\mathrm{Re}(\hat{E}_1^*\hat{E}_2)[p_1\cdot k_1p_2\cdot k_2+p_1\cdot k_2p_2\cdot k_1-k_1\cdot k_2(p_1\cdot p_2+M_N{}^2)]\}\\
&\quad+32\{|\hat{B}_1|^2(2p_1\cdot k_1p_2\cdot k_2+2p_1\cdot k_2p_2\cdot k_1-k_1\cdot k_2p_1\cdot p_2)\\
&\quad+|B_3|^2[-q^2(2p_1\cdot k_1p_2\cdot k_2+2p_1\cdot k_2p_2\cdot k_1-k_1\cdot k_2p_1\cdot p_2)\\
&\qquad+2p_2\cdot q(2p_1\cdot k_1q\cdot k_2+2p_1\cdot k_2q\cdot k_1-k_1\cdot k_2p_1\cdot q)]\\
&\quad+|B_4|^2[-q^2(2p_1\cdot k_1p_2\cdot k_2+2p_1\cdot k_2p_2\cdot k_1-k_1\cdot k_2p_1\cdot p_2)+2p_1\cdot q(2p_2\cdot k_1q\cdot k_2+2p_2\cdot k_2q\cdot k_1-k_1\cdot k_2p_2\cdot q)]\\
&\quad+2M_N\mathrm{Re}(\hat{B}_1^*B_3)(2k_1\cdot qk_2\cdot p_1+2k_2\cdot qk_1\cdot p_1-p_1\cdot qk_1\cdot k_2)\\
&\quad+2M_N\mathrm{Re}(\hat{B}_1^*B_4)(2k_1\cdot qk_2\cdot p_2+2k_2\cdot qk_1\cdot p_2-p_2\cdot qk_1\cdot k_2)+2M_N{}^2\mathrm{Re}(B_3^*B_4)(4q\cdot k_1q\cdot k_2-k_1\cdot k_2q^2)\}\\
&\quad+16\{-\mathrm{Re}(A_1^*\hat{B}_1)(k_1\cdot p_1k_2\cdot p_2-k_1\cdot p_2k_2\cdot p_1)+M_N\mathrm{Re}[A_1^*(B_3-B_4)](k_1\cdot qk_2\cdot P-k_1\cdot Pk_2\cdot q)\\
&\quad+\mathrm{Re}(\hat{A}_2^*\hat{B}_1)(k_1\cdot p_1k_2\cdot p_2-k_1\cdot p_2k_2\cdot p_1)+\mathrm{Re}[\hat{A}_2^*(B_3+B_4)]M_Nk_1\cdot k_2K\cdot q-\mathrm{Re}(A_3^*\hat{B}_1)M_Nk_1\cdot k_2q\cdot K\\
&\quad+\mathrm{Re}(A_3^*B_3)[q^2(k_1\cdot p_1k_2\cdot p_2-k_1\cdot p_2k_2\cdot p_1)-2p_2\cdot q(k_1\cdot p_1k_2\cdot q-k_1\cdot qp_1\cdot k_2)]\\
&\quad+\mathrm{Re}(A_3^*B_4)[q^2(k_1\cdot p_1k_2\cdot p_2-k_1\cdot p_2k_2\cdot p_1)+2p_1\cdot q(k_1\cdot p_2k_2\cdot q-k_1\cdot qp_2\cdot k_2)]\\
&\quad-\mathrm{Re}(C_1^*\hat{B}_1)M_Nk_1\cdot k_2k\cdot(q-k)\\
&\quad+\mathrm{Re}(C_1^*B_3)[M_N{}^2k_1\cdot k_2q\cdot k+k_1\cdot k_2(p_1\cdot qp_2\cdot k-p_2\cdot qp_1\cdot k-p_1\cdot p_2q\cdot k)\\
&\qquad-2p_1\cdot K(q\cdot k_2k_1\cdot p_2-p_2\cdot k_2k_1\cdot q)]\\
&\quad-\mathrm{Re}(C_1^*B_4)[M_N{}^2k_1\cdot k_2q\cdot k-k_1\cdot k_2(p_1\cdot qp_2\cdot k-p_2\cdot qp_1\cdot k+p_1\cdot p_2q\cdot k)\\
&\qquad-2p_2\cdot K(q\cdot k_2k_1\cdot p_1-p_1\cdot k_2k_1\cdot q)]\\
&\quad+\mathrm{Re}\,(C_2^*\hat{B}_1)4k_1\cdot k_2[p_1\cdot k_1p_2\cdot k_2+p_1\cdot k_2p_2\cdot k_1-\tfrac{1}{2}(p_1\cdot p_2+M_N{}^2)k_1\cdot k_2]\\
&\quad+2\,\mathrm{Re}(C_2^*B_3)M_Nk_1\cdot k_2[P\cdot k_1q\cdot k_2+P\cdot k_2q\cdot k_1+q\cdot k_1k_2\cdot(p_1-p_2)+q\cdot k_2k_1\cdot(p_1-p_2)-P\cdot qk_1\cdot k_2]\\
&\quad+2\,\mathrm{Re}(C_2^*B_4)M_Nk_1\cdot k_2[P\cdot k_1q\cdot k_2+P\cdot k_2q\cdot k_1-q\cdot k_1k_2\cdot(p_1-p_2)-q\cdot k_2k_1\cdot(p_1-p_2)-P\cdot qk_1\cdot k_2]\\
&\quad+2\,\mathrm{Re}(C_3^*\hat{B}_1)k_1\cdot k_2[k_1\cdot k_2(p_1\cdot p_2-M_N{}^2)-2(p_1\cdot k_1p_2\cdot k_2+p_1\cdot k_2p_2\cdot k_1)]\\
&\quad+2\,\mathrm{Re}(C_3^*B_3)M_Nk_1\cdot k_2[k_1\cdot k_2q\cdot(p_1-p_2)-2(p_1\cdot k_1q\cdot k_2+p_1\cdot k_2q\cdot k_1)]\\
&\quad+2\,\mathrm{Re}(C_3^*B_4)M_Nk_1\cdot k_2[-k_1\cdot k_2q\cdot(p_1-p_2)-2(p_2\cdot k_1q\cdot k_2+p_2\cdot k_2q\cdot k_1)]\\
&\quad+\mathrm{Re}(\hat{E}_1^*\hat{B}_1)M_Nk_1\cdot k_2k_1\cdot P-\mathrm{Re}(\hat{E}_2^*\hat{B}_1)M_Nk_1\cdot k_2k_2\cdot P\\
&\quad+\mathrm{Re}(\hat{E}_1^*B_3)[M_N{}^2k_1\cdot k_2k_1\cdot q-p_1\cdot k_1(2p_2\cdot k_2k_1\cdot q-2k_1\cdot p_2k_2\cdot q-p_2\cdot qk_1\cdot k_2)\\
&\qquad-k_1\cdot k_2(k_1\cdot p_2p_1\cdot q-p_1\cdot p_2q\cdot k_1)]
\end{aligned}
$$

$$
\begin{aligned}
&+\mathrm{Re}(\hat{E}_2^* B_3)[-M_N{}^2 k_1\cdot k_2 k_2\cdot q + p_1\cdot k_2(2k_1\cdot p_2 k_2\cdot q - 2p_2\cdot k_2 k_1\cdot q - p_2\cdot q k_1\cdot k_2)\\
&\qquad + k_1\cdot k_2(k_2\cdot p_2 p_1\cdot q - p_1\cdot p_2 q\cdot k_2)]\\
&+\mathrm{Re}(\hat{E}_1^* B_4)[M_N{}^2 k_1\cdot k_2 k_1\cdot q - p_2\cdot k_1(2p_1\cdot k_2 k_1\cdot q - 2k_1\cdot p_1 k_2\cdot q - p_1\cdot q k_1\cdot k_2)\\
&\qquad - k_1\cdot k_2(k_1\cdot p_1 p_2\cdot q - p_1\cdot p_2 q\cdot k_1)]\\
&+\mathrm{Re}(\hat{E}_2^* B_4)[-M_N{}^2 k_1\cdot k_2 k_2\cdot q + p_2\cdot k_2(2k_1\cdot p_1 k_2\cdot q - 2p_1\cdot k_2 k_1\cdot q - p_1\cdot q k_1\cdot k_2)\\
&\qquad + k_1\cdot k_2(k_2\cdot p_1 p_2\cdot q - p_1\cdot p_2 q\cdot k_2)]\}\\
&+8\epsilon_{\alpha\beta\gamma\delta} p_1^\alpha p_2^\beta k_1^\gamma k_2^\delta\{-2\,\mathrm{Im}(A_1^* C_3)k_1\cdot k_2 - 2\,\mathrm{Im}(\hat{A}_2^* C_2)k_1\cdot k_2 + \mathrm{Im}[A_3^*(\hat{E}_1+\hat{E}_2)]k_1\cdot k_2\\
&\qquad - \mathrm{Im}[C_1^*(\hat{E}_1-\hat{E}_2)]k_1\cdot k_2 + 2\,\mathrm{Im}(A_1^*\hat{B}_1) - 4M_N\mathrm{Im}[A_1^*(B_3-B_4)] - 2\,\mathrm{Im}(\hat{A}_2^* B_1)\\
&\qquad - 2(q^2+2p_2\cdot q)\mathrm{Im}(A_3^* B_3) - 4p_1\cdot K\,\mathrm{Im}(C_1^* B_3) + 4p_2\cdot K\,\mathrm{Im}(C_1^* B_4)\\
&\qquad + 2k_1\cdot(p_1+p_2+q)\mathrm{Im}(\hat{E}_1^* B_3) + 2k_2\cdot(p_1+p_2+q)\mathrm{Im}(\hat{E}_2^* B_3) + 2k_1\cdot(p_1+p_2-q)\mathrm{Im}(\hat{E}_1^* B_4)\\
&\qquad + 2k_2\cdot(p_1+p_2-q)\mathrm{Im}(\hat{E}_2^* B_4) - 2(q^2-2p_1\cdot q)\mathrm{Im}(A_3^* B_4)\}, \qquad \text{(A5)}
\end{aligned}
$$

where $P = p_1 + p_2$, $k = k_1 - k_2$, and $K = k_1 + k_2$.

APPENDIX B: APPROXIMATE CALCULATION OF (3,3)-RESONANCE EXCITATION

To calculate the effect of (3, 3)-resonance excitation in weak-pion production induced by S, P, T isovector currents, we use two methods. As a first approximation, we evaluate the (3, 3) excitation matrix element in the static limit using a variant of the method first developed for photoproduction by Chew and Low.[20] In this limit, the scalar current does not contribute. A more accurate treatment of (3, 3) excitation requires projecting out the (3, 3) multipoles appropriate to S, P, T currents. While the work involved in a complete projection for the tensor current is prohibitive, the scalar and pseudoscalar calculation is easily done. Therefore we use the multipole projection method to evaluate the (3, 3) excitation matrix elements induced by the scalar current and the pseudoscalar current, using the latter as a check against the static-model calculation. Combining this result with that obtained from the static model gives the leading nonvanishing approximation to the (3, 3)-resonance excitation matrix element in the S, P, T case.

The basic idea of the static model may be described succinctly as follows. We start by considering the pion-nucleon scattering process $\pi^i(k) + N(p_1) \to \pi(q) + N(p_2)$, for which the resonant matrix element in the center-of-mass frame may be written as

$$
\mathfrak{M} = 4\pi\chi_{s2}^\dagger(3\vec{q}-\vec{\sigma}\cdot\vec{q}\,\vec{\sigma})\cdot\vec{k}\chi_{s1}\frac{f_{1^+}^{(3/2)}}{|\vec{q}|^2}a^{(3/2)},
$$

$$
a^{(3/2)} = \chi_2^\dagger\psi_j^*[\Pi^{3/2}]_{jl}\chi_1\psi_{il},
$$

$$
\Pi_{jl}^{(3/2)} = \tfrac{1}{3}\{\tau_j,\tau_l\}_+ - \tfrac{1}{6}[\tau_j,\tau_l], \qquad \text{(B1)}
$$

$$
f_{1^+}^{(3/2)} \equiv e^{i\delta_{3,3}}\sin\delta_{3,3}/|\vec{q}|,
$$

with χ_{s2}, χ_{s1} being the final and initial nucleon spinors, χ_2, χ_1 being the final and initial nucleon isospinors, and ψ and ψ_i being the final and initial pion isospin wave functions. This scattering amplitude may be thought of as arising from resonant rescattering of the outgoing pion coming from the crossed nucleon Born diagram, as illustrated in Fig. 9(a). What we want to evaluate is the corresponding pion-production diagram with an S, P, T neutral-current incident instead of a pion, as illustrated in Fig. 9(b). (The s-channel Born diagrams contribute only to $I = \frac{1}{2}$ amplitudes, and so make no contribution to resonant pion production in either case.) The static model relates the two processes of Fig. 9(a) and Fig. 9(b) by regarding them as resulting from the action of the same linear operator acting, respectively, on the static-nucleon limit of the pion-nucleon or current-nucleon vertex. A simple calculation shows that the static-nucleon limit of the pion-nucleon vertex appearing in Fig. 9(a) is

$$
\bar{u}(p_2)\gamma_5 g_r\tau_l u(p_1)\psi_{il} \xrightarrow[\text{limit}]{\text{static}} \left(\frac{-g_r}{2M_N}\right)\chi_{s2}^\dagger\vec{\sigma}\cdot\vec{k}\chi_{s1}\chi_2^\dagger\tau_l\chi_1\psi_{il}, \qquad \text{(B2)}
$$

permitting us to identify the linear operator by comparison with Eq. (B1). Taking then the static-nucleon limit[38] of the current-nucleon vertex appearing in Fig. 9(b),

$$\frac{G}{\sqrt{2}}\Big\{\bar{\nu}(1-\gamma_5)\nu\bar{u}(p_2)[g_{S3}F_S^{(3)}(k^2)+g_{P3}F_P^{(3)}(k^2)\gamma_5]\tfrac{1}{2}\tau_3 u(p_1)$$
$$+\bar{\nu}\sigma_{\lambda\eta}(1-\gamma_5)\nu\bar{u}(p_2)\,g_{T3}\Big[T_1^{(3)}(k^2)\sigma^{\lambda\eta}+\frac{iT_2^{(3)}(k^2)}{M_N}(\gamma^\lambda k^\eta-\gamma^\eta k^\lambda)+\frac{iT_3^{(3)}(k^2)}{M_N{}^2}(P^\lambda k^\eta-P^\eta k^\lambda)\Big]\tfrac{1}{2}\tau_3 u(p_1)\Big\}$$
$$\xrightarrow[\text{limit}]{\text{static}}\chi_{s2}^\dagger\vec{\sigma}\cdot\vec{v}\chi_{s1}\chi_2^\dagger\tau_i\chi_1(\tfrac{1}{2}\delta_{i3})+\text{terms proportional to }\chi_{s2}^\dagger\chi_{s1}\text{ [which do not excite the (3, 3) resonance]},\tag{B3}$$

we can immediately identify the pion-production matrix element as

$$\mathfrak{M}_\pi^{\text{static}}=-\frac{8\pi M_N}{g_r}\frac{f_{1+}^{(3/2)}}{|\vec{q}|^2}\chi_{s2}^\dagger(3\vec{q}-\vec{\sigma}\cdot\vec{q}\,\vec{\sigma})\cdot\vec{v}\chi_{s1}a_E^{(3/2)},$$

$$a_E^{(3/2)}=\chi_2^\dagger\psi_f^\dagger[\pi^{(3/2)}]_{fi}\chi_1\tfrac{1}{2}\delta_{i3},\tag{B4}$$

with $a_E^{(3/2)}$ being the isospin matrix element tabulated in the final column of Table I, and with $\vec{v}$ given by

$$\vec{v}=-ag_{P3}F_P^{(3)}(k^2)\frac{\vec{k}}{2M_N}-2iag_{T3}\frac{T_2^{(3)}(k^2)}{M_N{}^2}(\vec{k}_1\times\vec{k}_2)$$
$$+2\vec{b}g_{T3}T_1^{(3)}(k^2).\tag{B5}$$

The quantities a and $\vec{b}$ appearing in Eq. (B5) are leptonic matrix elements, which may be written in terms of the isobaric-frame kinematic quantities defined in Fig. 10 as

$$a=\frac{G}{\sqrt{2}}\bar{\nu}(1-\gamma_5)\nu$$
$$=\frac{G}{\sqrt{2}}\frac{(k_{10}k_{20})^{1/2}}{2m_\nu}4\sin(\tfrac{1}{2}\theta),$$
$$\vec{b}=\frac{G}{\sqrt{2}}\bar{\nu}\vec{\sigma}(1-\gamma_5)\nu\tag{B6}$$
$$=\frac{G}{\sqrt{2}}\frac{(k_{10}k_{20})^{1/2}}{2m_\nu}\frac{2}{\sin(\frac{1}{2}\theta)}(\hat{k}_2-\hat{k}_1-i\hat{k}_1\times\hat{k}_2).$$

As we have already noted, Eq. (B5) contains no scalar contribution. To get the leading nonvanishing scalar contribution to the matrix element we use the multipole expansion method,

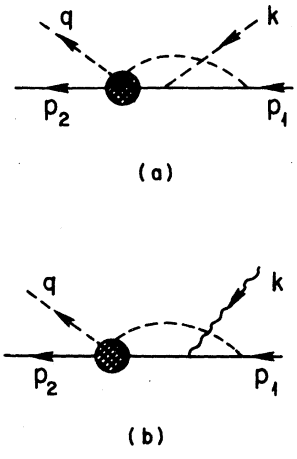

FIG. 9. Diagrams describing the contribution of the crossed nucleon Born diagram, with resonant final-state rescattering, to (a) pion-nucleon scattering and (b) current-induced pion production. The wavy line denotes the incident current.

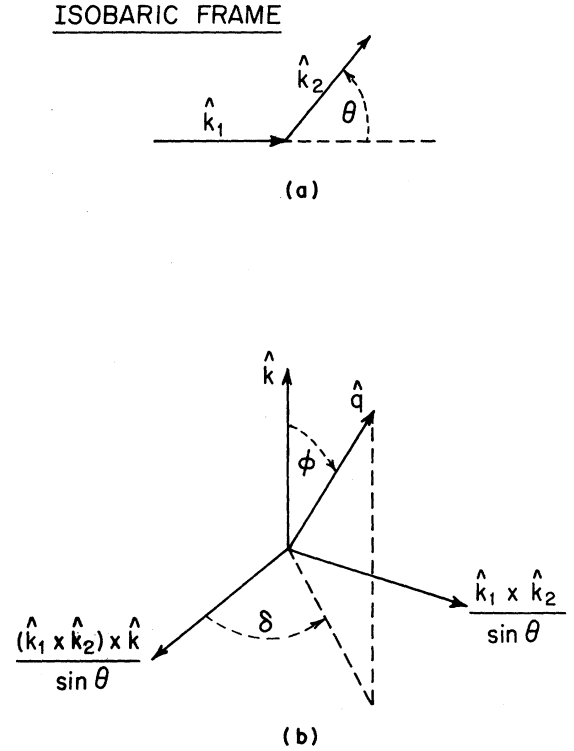

FIG. 10. (a) Isobaric frame angle between the initial and final neutrino directions. (b) Axes and angles which specify the final pion direction $\hat{q}$ in the isobaric frame, with $\hat{k}$ being the direction of the momentum transfer between the neutrinos.

carrying along the pseudoscalar (but not the tensor) term as a check. We begin by isolating the $I=\frac{3}{2}$ parts of the scalar- and pseudoscalar-interaction pion-production matrix elements, and by writing for them a general invariant decomposition between nucleon spinors,

$$\begin{aligned}
&\mathfrak{M}_\pi^S = a_E^{(1/2)} S^{(1/2)} + a_E^{(3/2)} S^{(3/2)},\\
&\mathfrak{M}_\pi^P = a_E^{(1/2)} P^{(1/2)} + a_E^{(3/2)} P^{(3/2)},\\
&S^{(3/2)} = a\,\bar{u}(p_2)[A\gamma_5 + B(\not{q}+\not{k})\gamma_5]u(p_1),\\
&P^{(3/2)} = a\,\bar{u}(p_2)[C + D(\not{q}+\not{k})]u(p_1),
\end{aligned} \tag{B7}$$

with $a_E^{(1/2,3/2)}$ as tabulated in Table I and with a being the lepton matrix element of Eq. (B6). The Born-approximation contributions to $A,\ldots,D$ may be read off from Eq. (19a) of the text,

$$\begin{aligned}
&A^B = -g_{S3} F_S^{(3)}(k^2) \frac{g_r}{\nu+\nu_B},\\
&B^B = g_{S3} F_S^{(3)}(k^2) \frac{g_r}{2M_N(\nu+\nu_B)},\\
&C^B = 0,\\
&D^B = -g_{P3} F_P^{(3)}(k^2) \frac{g_r}{2M_N(\nu+\nu_B)}.
\end{aligned} \tag{B8}$$

We introduce multipole expansions for $S^{(3/2)}$, $P^{(3/2)}$ by writing

$$\begin{aligned}
S^{(3/2)} &= \chi_{s2}^\dagger \sum_{l=0}^{\infty} (2l+1)(\Pi_{l+}^S h_{l+}^{(3/2)} + \Pi_{l-}^S h_{l-}^{(3/2)})\\
&\quad \times P_l(\cos\phi)\chi_{s1},\\
P^{(3/2)} &= \chi_{s2}^\dagger \sum_{l=0}^{\infty} (2l+1)(\Pi_{l+} g_{l+}^{(3/2)} + \Pi_{l-} g_{l-}^{(3/2)})\\
&\quad \times P_l(\cos\phi)\chi_{s1},
\end{aligned} \tag{B9}$$

with ϕ the pion-current angle defined in Fig. 10 and with the scalar-current transition operators $\Pi_{l\pm}^S$ related to the angular momentum projection operators $\Pi_{l\pm}$ by a Minami transformation,

$$\begin{aligned}
&\Pi_{l+}^S = \vec{\sigma}\cdot\hat{q}\,\Pi_{l+},\quad \Pi_{l-}^S = \vec{\sigma}\cdot\hat{q}\,\Pi_{l-},\\
&\Pi_{l+} = \frac{l+1+\vec{\sigma}\cdot\vec{L}}{2l+1},\quad \Pi_{l-} = \frac{l-\vec{\sigma}\cdot\vec{L}}{2l+1}.
\end{aligned} \tag{B10}$$

Carrying out the differentiations implicit in the angular momentum operator $\vec{L}$ acting on the Legendre polynomials, Eq. (B9) gives

$$\begin{aligned}
S^{(3/2)} &= \chi_{s2}^\dagger \sum_{l=0}^{\infty} \{[(l+1)h_{l+}^{(3/2)} + l h_{l-}^{(3/2)}]\vec{\sigma}\cdot\hat{q} P_l(\cos\phi) + (\vec{\sigma}\cdot\hat{k} - \cos\phi\,\vec{\sigma}\cdot\hat{q})(h_{l-}^{(3/2)} - h_{l+}^{(3/2)})P_l'(\cos\phi)\}\chi_{s1},\\
P^{(3/2)} &= \chi_{s2}^\dagger \sum_{l=0}^{\infty} \{[(l+1)g_{l+}^{(3/2)} + l g_{l-}^{(3/2)}]P_l(\cos\phi) + i\vec{\sigma}\cdot(\hat{q}\times\hat{k})(g_{l-}^{(3/2)} - g_{l+}^{(3/2)})P_l'(\cos\phi)\}\chi_{s1}.
\end{aligned} \tag{B11}$$

Using standard Legendre polynomial identities to invert Eq. (B10), the multipole amplitudes can be expressed in terms of the invariant amplitudes:

$$\begin{aligned}
h_{l\pm}^{(3/2)} &= \frac{O_{1+}}{2M_N} a^{\frac{1}{2}} \int_{-1}^{1} dz \left[(A-2WB)\left(\frac{p_{20}-M_N}{p_{20}+M_N}\right)^{1/2} P_l(z) - (A+2WB)\left(\frac{p_{10}-M_N}{p_{10}+M_N}\right)^{1/2} P_{l\pm1}(z)\right],\\
g_{l\pm}^{(3/2)} &= \frac{O_{1+}}{2M_N} a^{\frac{1}{2}} \int_{-1}^{1} dz \left\{[C+2(W-M_N)D]P_l(z) + [-C+2(W+M_N)D]\left(\frac{p_{10}-M_N}{p_{10}+M_N}\right)^{1/2}\left(\frac{p_{20}-M_N}{p_{20}+M_N}\right)^{1/2} P_{l\pm1}(z)\right\},\\
O_{1+} &= [(p_{10}+M_N)(p_{20}+M_N)]^{1/2}.
\end{aligned} \tag{B12}$$

Substituting the Born approximation of Eq. (B8) into Eq. (B12) we find

$$\begin{aligned}
h_{1+}^{(3/2)B} &= -\frac{O_{1+}}{2M_N} a \frac{g_{S3} F_S^{(3)}(k^2) g_r}{|\vec{q}|\,|\vec{k}|}\left[-(M_N+W)\left(\frac{p_{20}-M_N}{p_{20}+M_N}\right)^{1/2} Q_1(\beta) + (M_N-W)\left(\frac{p_{10}-M_N}{p_{10}+M_N}\right)^{1/2} Q_2(\beta)\right],\\
g_{1+}^{(3/2)B} &= \frac{O_{1+}}{2M_N} a \frac{g_{P3} F_P^{(3)}(k^2) g_r}{|\vec{q}|\,|\vec{k}|}\left[(W-M_N)Q_1(\beta) + (W+M_N)\left(\frac{p_{10}-M_N}{p_{10}+M_N}\right)^{1/2}\left(\frac{p_{20}-M_N}{p_{20}+M_N}\right)^{1/2} Q_2(\beta)\right],\\
\beta &= (-2p_{20}k_0 + k^2)/(2|\vec{q}|\,|\vec{k}|)\ \text{(Ref. 39)}.
\end{aligned} \tag{B13}$$

Taking the static limit, in which $\beta\to-\infty$, Eq. (B13) then yields

$$\begin{aligned}
h_{1+}^{(3/2)B} &\approx a g_{S3} F_S^{(3)}(k^2) g_r \frac{|\vec{q}|^2|\vec{k}|}{3\omega^2 M_N^2},\\
g_{1+}^{(3/2)B} &\approx a g_{P3} F_P^{(3)}(k^2) g_r \frac{|\vec{q}|\,|\vec{k}|}{3\omega M_N^2}.
\end{aligned} \tag{B14}$$

Finally, using the unitarization procedure described in the text we get for the resonant scalar and pseudoscalar pion-production multipoles

$$h_{1+}^{(3/2)} = h_{1+}^{(3/2)B}\, s,\quad g_{1+}^{(3/2)} = g_{1+}^{(3/2)B}\, r, \tag{B15}$$

with r defined in Eq. (28) of the text, and with $s=r$ or $s=\cos\delta_{3,3}$ depending on whether the scalar

amplitude is unitarized according to the procedures of Eq. (27) or Eq. (30), respectively.

Combining Eqs. (B14)–(B15) with Eqs. (B11) and (B7) we find the resonant pion-production matrix element:

$$\mathfrak{M}_\pi^P = a_E^{(3/2)} \chi_{s2}^\dagger (3\vec{q} - \vec{\sigma}\cdot\vec{q}\,\vec{\sigma})\cdot\vec{w}_P \chi_{s1} \frac{2}{3}\frac{g_r}{M_N\omega} r,$$

$$\mathfrak{M}_\pi^S = a_E^{(3/2)} \chi_{s2}^\dagger (3\vec{q} - \vec{\sigma}\cdot\vec{q}\,\vec{\sigma})\cdot\vec{w}_S \chi_{s1} \frac{2}{3}\frac{g_r}{M_N\omega} s, \tag{B16}$$

$$\vec{w}_P = a g_{P3} F_P^{(3)}(k^2)\frac{\vec{k}}{2M_N},$$

$$\vec{w}_S = a g_{S3} F_S^{(3)}(k^2)\frac{\vec{\sigma}\cdot\vec{q}\,\vec{k} + 2i\vec{q}\times\vec{k}}{2M_N\omega}.$$

Using the identity

$$\frac{2}{3}\frac{g_r}{M_N\omega} r = \frac{8\pi M_N}{g_r}\frac{f_{1+}^{(3/2)}}{|\vec{q}|^2}, \tag{B17}$$

we immediately see that $\mathfrak{M}_\pi^P$ of Eq. (B16) is identical to the pseudoscalar term in the static expression of Eqs. (B4)–(B5), as expected. Hence we identify

$$\mathfrak{M}_\pi^{S,P,T} = \mathfrak{M}_\pi^{\text{static}} + \mathfrak{M}_\pi^S \tag{B18}$$

as the leading approximation to the complete resonant pion-production matrix element. Squaring, spin-averaging, and integrating over pion angular variables yields in a straightforward manner Eq. (31) of the text.[40]

---

*Research sponsored in part by the U. S. Atomic Energy Commission, Grant No. AT(11-1)-2220.

[1]S. Weinberg, Phys. Rev. Lett. 19, 1264 (1967); A. Salam, in *Elementary Particle Theory: Relativistic Groups and Analyticity (Nobel Symposium No. 8)*, edited by N. Svartholm (Almqvist and Wiksell, Stockholm, 1968), p. 367; S. Weinberg, Phys. Rev. D 5, 1412 (1972).

[2]See, for example, B. Kayser *et al.*, Phys. Lett. B52, 385 (1974); R. L. Kingsley *et al.*, Phys. Rev. D 10, 2216 (1974).

[3]F. J. Hasert *et al.*, Phys. Lett. 46B, 138 (1973); A. Benvenuti *et al.*, Phys. Rev. Lett. 32, 800 (1974).

[4]S. L. Adler, Phys. Rev. D (to be published).

[5]S. L. Adler, E. W. Colglazier, Jr., J. B. Healy, I. Karliner, J. Lieberman, Y. J. Ng, and H.-S. Tsao, Phys. Rev. D 11, 3309 (1975).

[6]S. L. Adler, R. F. Dashen, J. B. Healy, I. Karliner, J. Lieberman, Y. J. Ng, and H.-S. Tsao, following paper, Phys. Rev. D 12, 3522 (1975).

[7]We follow throughout the metric and γ-matrix conventions of J. D. Bjorken and S. D. Drell, *Relativistic Quantum Fields* (McGraw-Hill, New York, 1965), Appendix A. Also, throughout this paper ν will be understood to mean a muon neutrino ν_μ.

[8]See R. L. Kingsley *et al.*, Ref. 2.

[9]A succinct review is given in O. Nachtmann, Nucl. Phys. B38, 397 (1972). See also R. P. Feynman, *Photon Hadron Interactions* (Benjamin, New York, 1972).

[10]See, for example, L. M. Sehgal, Nucl. Phys. B65, 141 (1973).

[11]The scaling variables x, y are conventionally defined by $x = -k^2/2k\cdot p_N$, $y = 1 - E_2/E$, with k being the virtual current four-momentum, p_N being the target nucleon four-momentum, and E_2 and E the outgoing lepton and incident neutrino lab energies. For a detailed discussion of deep-inelastic neutrino scattering in the S, P, T coupling case, see S. Pakvasa and G. Rajasekaran, Phys. Rev. (to be published).

[12]G. F. Chew, M. L. Goldberger, F. E. Low, and Y. Nambu, Phys. Rev. 106, 1345 (1957); S. Fubini, Y. Nambu, and V. Wataghin, *ibid.* 111, 329 (1958).

[13]A comparison of the CGLN model with pion photoproduction data is given by G. Höhler and W. Schmidt, Ann. Phys. (N.Y.) 28, 34 (1964); W. Schmidt, Z. Phys. 182, 76 (1964). Comparisons in the electroproduction case are given by S. L. Adler, Ann. Phys. (N. Y.) 50, 189 (1968).

[14]For comparisons in the weak production case, see S. L. Adler, Ref. 4, and P. A. Schreiner and F. von Hippel, Argonne National Laboratory Report No. ANL/HEP 7309.

[15]See, for example, S. L. Adler and R. F. Dashen, *Current Algebras* (Benjamin, New York, 1968).

[16]For a more detailed discussion, see S. L. Adler and W. I. Weisberger, Phys. Rev. 169, 1392 (1968).

[17]The fact that Eq. (17) is of first order in the pion four-momentum q is a consequence of the fact that the zeroth-order terms in q are *uniquely* determined by the soft-pion formula, Eq. (12).

[18]S. L. Adler, Ann. Phys. (N.Y.) 50, 189 (1968). Note that this reference employs different metric and γ-matrix conventions from those of the present paper.

[19]The parameterization for $\exp(i\delta_{3,3})\sin\delta_{3,3}$ is due to L. D. Roper, Phys. Rev. Lett. 12, 340 (1964).

[20]G. F. Chew and F. E. Low, Phys. Rev. 101, 1579 (1956); J. S. Bell and S. M. Berman, Nuovo Cimento 25, 404 (1962).

[21]The (unitarized) contribution of the tensor pion-pole diagram of Fig. 1(a) is neglected in the static-model estimate of resonant pion production.

[22]R. L. Kingsley, R. Shrock, S. B. Treiman, and F. Wilczek, Phys. Rev. D 11, 1043 (1975).

[23]Columbia-Illinois-Rockefeller collaboration, data presented at the Weak Interactions Symposium, Paris, 1974 (unpublished). The error ± 0.06 includes systematic uncertainties; the statistical error is considerably smaller.

[24]S. L. Adler, S. Nussinov, and E. A. Paschos, Phys. Rev. D 9, 2125 (1974).

[25]See S. L. Adler, Ref. 4, Table III.

[26]F. J. Hasert *et al.*, report to the XVII International Conference on High Energy Physics, London, 1974 (unpublished).

[27]B. Aubert *et al.*, Phys. Rev. Lett. 32, 1454 (1974); 32, 1457 (1974); and report to the Symposium on Neutral Currents, Argonne National Laboratory, 1975 (unpublished).

[28]B. C. Barish *et al.*, Phys. Rev. Lett. 34, 538 (1975).

[29]F. Sciulli, Caltech-Fermilab experiment (private communication).

[30]D. C. Cundy *et al.*, Phys. Lett. 31B, 478 (1970).

[31]The BNL flux table has been furnished to us by W. Y. Lee and L. Litt (private communication). The CERN neutrino flux is given by D. H. Perkins, in *Proceedings of the Fifth Hawaii Topical Conference in Particle Physics, 1973*, edited by P. N. Dobson, Jr., V. Z. Peterson, and S. F. Tuan, (Univ. of Hawaii Press, Honolulu, 1974), Fig. 1.6. Note that the absolute magnitude of the flux is irrelevant in flux averaging—only the shape of the spectrum matters.

[32]In doing the computational work in the S, P, T case, we have used the same quadratic form method used in the V, A case in Ref. 4.

[33]In addition to being the dipole mass suggested by the quark model, $M \approx 0.9$ GeV is also roughly the dipole mass which occurs in the measured vector and axial-vector form factors.

[34]For a given choice of coupling *ratios* $g_{S0}:g_{P0}:g_{T0}$ and of renormalization parameters, the pion-production upper bound is determined by rescaling the over-all strength of the weak neutral current to the maximum value compatible with the constraints of Eqs. (37) and (39).

[35]See J. D. Jackson, in *Elementary Particle Physics and Field Theory*, 1962 Brandeis Summer Institute in Theoretical Physics, edited by K. W. Ford (Benjamin, New York, 1963), p. 280. Note that Jackson's notation and kinematic conventions differ from ours.

[36]Talking about ep and μp interactions of course presupposes an extension of the effective Lagrangian of Eq. (2) to include terms for e-hadron and μ-hadron, as well as ν-hadron, neutral interactions.

[37]This qualitative behavior of the scalar isovector current results from the fact that (3, 3) resonance production is governed by $F_S^{(3)}(0)$, which is relatively small, while through the equal-time commutator term the branching ratios are influenced by the renormalization constants $F_P^{(0)}(0)$ and $F_P^{(3)}(0)$, which are not small.

[38]In taking the static limit, terms proportional to $(\vec{p}_2 - \vec{p}_1)/M_N = \vec{k}/M_N$, which can be referred back to variables of the incident current, are retained, but nucleon recoil terms proportional to $(\vec{p}_2 + \vec{p}_1)/M_N$ are dropped. See J. S. Bell and S. M. Berman, Ref. 20, for a further discussion of this and related points.

[39]The associated Legendre polynomials $Q_l(\beta)$ are defined in *Higher Transcendental Functions* (Bateman Manuscript Project) edited by A. Erdélyi (McGraw-Hill, New York, 1953), Vol. I, p. 154, Eq. (29).

[40]The scalar-tensor interference term makes no contribution to the total cross section because it is odd in $\vec{q}$, and hence vanishes when integrated over pion angle. Note that the appearance of $3\vec{q} - \vec{\sigma} \circ \vec{q}\vec{\sigma}$ in the scalar matrix element of Eq. (B16) is expected because this quantity is the isobaric frame limit of the spin-$\frac{3}{2}$ Rarita-Schwinger spinor. However, since the vector $\vec{w}_S$ is proportional to $\vec{q}$, rather than being $\vec{q}$ independent (as is the case for $\vec{w}_P$), the scalar amplitude is not determined by the static-model argument.